	Cu %	S %
a–3129	0.44	0.16
a–3130	11.15	0.28
3–3131	0.47	0.07

In these, most of the copper is derived from secondary minerals including malachite. Microscopic observation of sample a–3130 showed the secondary copper minerals and small amount of pyrite as ore minerals in which sulfides were hardly observed, but the sample contained minute grains of molybdenite.

The distance between this outcrop and MA–3 mentioned above is 300 m, and the relation between them has not been known because of thick vegetation.

(4) MA–5 Outcrop

It is a small outcrop in quartz diorite with the extent of 2 m x 1 m located 200 m northwest of MA–4 outcrop. Granodiorite stock is found about 30 m west of the outcrop. The outcrop consists of thick dissemination of pyrite, in which copper mineral is entirely absent.

Although there is a test pit excavated toward the center of outcrop in the direction of N 55°W, the pit could not be well observed because of the collapse materials at the entrance. A lump sample of pyrite dissemination (a–3132) showed assays of 0.45% Cu and 0.12% S.

Drilling hole BM·No. 3 (120.50 m) is located 100 m east of the outcrop and BM·No. 5 (the length is unknown) 100 m to the northwest. Although BM·No. 5 did not encounter the mineraliization, the following mineralization was confirmed through BM·No. 3. Sampling interval is the same to BM·No. 2.

Depth (m)	Length of sections (m)	Cu %
16.70 ∿ 25.85	9.15	0.38
33.45 ∿ 48.65	7.60	0.55
41.05 ∿ 48.65	7.60	1.05
48.65 ∿ 60.80	12.15	0.43
72.95 ∿ 86.65	13.70	0.43
86.65 ∿ 98.80	12.15	0.63
98.80 ∿ 106.40	7.60	4.53
110.95 ∿ 118.55	7.60	0.47

As shown above, a good copper mineralization was intersected in BM·No. 3. The grade at the section of 98.80 ∿ 106.40 m is very high for dissemination type copper deposit and

is considered to be the vein type deposit rich in copper mineral. The characteristics such as a kind of ore minerals, occurrence, and alteration of country rock are unknown because of absence of data.

Other three holes are situated surrounding BM·No. 3 in the center, such as BM·No. 5 mentioned above 180 m to the west, BM·No. 6,200 m to the east, and BM No. 4,200 m to the north, none of which showed ore intersection.

On the other hand, although BM·No. 3 is located on the Line-C of the IP survey, no IP anomaly was detected in the proximity. Therefore, it can be judged that the mineralization with abundant copper encountered by the drill hole is very local, having small lateral extension.

(5) MA–6 Outcrop

The outcrop located on the east bank in the middle stream of the Mamising Creek is, as shown in Fig. I–4, vein type within andesite lava.

The vein has the N 35°W strike, dip of 68°E and width of 10 cm, consisting mainly of massive ore of pyrite and chalcopyrite contained in the abundant hematite and clay. A small amount of malachite occurred along the periphery of the vein on the foot-wall.

In addition to the strong silicification and chloritization of andesite as host rock, it was argillized along the boundary with the vein. The irregular veinlets of quartz-calcite fills the small cracks in andesite.

From the results of X-ray diffractive analysis of the clay (a–3144) sampled from the vein, abundant quartz, chlorite and sericite were detected.

The result of analysis of ore samples cut from the massive pyrite-chalcopyrite-hematite ore (a–3143) is as follows:

	Details of Sample	Cu %	8 %	Fe %	Au g/t	Ag g/t
a–3143(a)	High grade part of chalcopyrite	27.87	22.41	–	0.1	51.9
a–3143(b)	Hematite ore	5.93	0.12	23.55	–	–
a–3143(c)	High grade part of chalcopyrite	11.37	10.68	–	–	–
a–3143(d)	Hematite	8.00	7.25	38.04	–	–

Under the microscope, samples a–3143(a) and a–3143(c) consist of massive chalcopyrite, in which secondary covellite was formed as filling of numerous cracks and tiny openings in reticular form in chalcopyrite. Minute hematite crystals are also observed in gangue mineral (quartz) in small amount. Although silver grade was as high as 51.9 g/t in a–3143(a), silver

mineral was not observed. Sample a–3143(b) consists of aggregate of lamella hematite considered to be primary, with partial development of secondary hematite. As mentioned above, the vein through small in width is high grade, containing abundant chalcopyrite. However, its occurrence and continuation have not been made clear because of the small exposure. The vein is quite different from the outcrops of dissemination-network type deposits and the relation between them is very interesting. However, such relation could not be made clear since there was no exposure between the two outcrops.

Drill hole BM·No. 1 is located midway between the outcrop and BM·No. 5. In this hole copper mineralization was very weak having shown average copper grade of 0.34% for the 3 m section at depth specifically from 48.65 m to 51.65 m in depth.

(6) MA–7 Outcrop

The outcrop is situated about 100 m south of MA–6, and it is, as shown in Fig. I–5, a dissemination-fine network zone formed along the boundary between quartz diorite and andesite lava.

The constituent minerals are malachite and very small amount of pyrite, and these occur in both quartz diorite and andesite in the form of dissemination, being more predominant in quartz diorite. Veinlets of white clay can be observed along the boundary of the host rock, in which a small amount of malachite is observed. The country rocks are both strongly silicified, chloritized and partly argillized.

The result of analysis of samples taken from the places as shown in Fig. I–5, such as three channel samples (a–3145, a–3146, a–3147), sample of clayey vein (a–3148), lump ore in quartz diorite (a–3149) and lump ore in andesite (a–3151), is as follows:

No.	Sampling width (m)	Cu %	S %	Au g/t	Ag g/t
a–3145	1.50	0.43	0.06	0.0	1.2
a–3146	1.50	0.32	0.08	0.0	0.5
a–3147	0.80	0.32	0.07	0.0	0.5
a–3148	(lump)	0.87	0.04	–	–
a–3149	(lump)	0.49	0.04	–	–
a–3151	(lump)	0.08	0.06	–	–

As shown above, the Cu content of almost same grade were obtained in channel sampling. However, the copper grade become abruptly lower in andesite 3–4 m from the boundary, and becomes strongly mineralized in quartz diorite.

At the boundary between quartz diorite and brecciated andesite lava about 70 m to

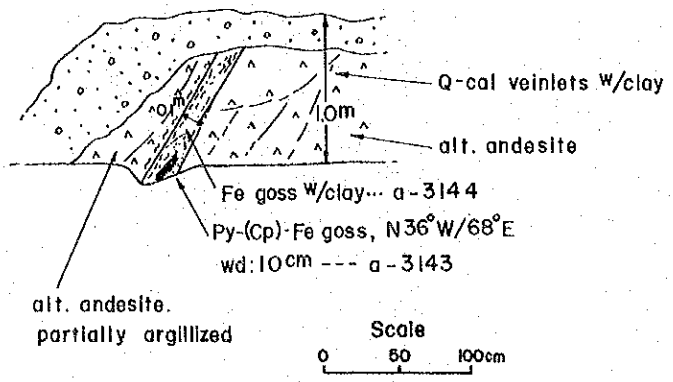

Fig. I–4 Sketch of MA–6 Mineralized Outcrop

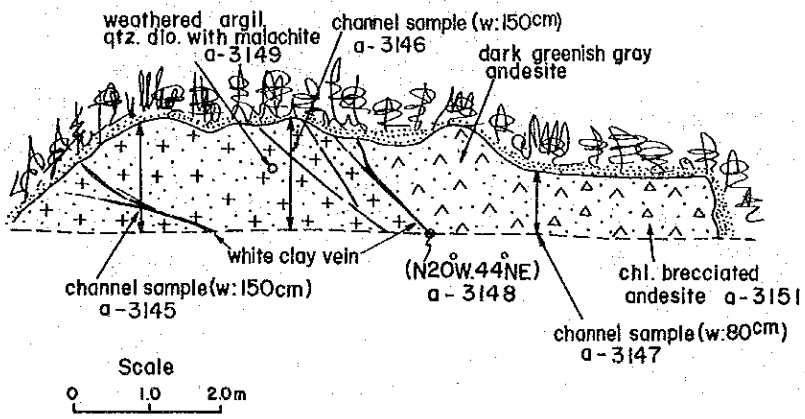

Fig. I–5 Sketch of MA–7 Mineralized Outcrop

the south of the outcrop, dissemination of malachite and small amount of pyrite is observed in both rocks though inferior compared with MA–7 outcrop.

The result of analysis of a lump ore sample, a mineralized rock with malachite dissemination in andesite, gave the values of 0.24% Cu and 0.42% S. X-ray diffractive analysis of the andesite showed that the rock underwent sericitization.

(7) MB–1 Outcrop

The outcrop is situated on the main stream of the Agalo Creek (middle to upper stream of the Mamising Creek is called the Agalo Creek), 450 m to the north of MA–5 outcrop. It is a pyrite dissemination zone formed along the northern periphery of the granodiorite stock. Although no copper mineral was observed by naked eye, the assay of the lump ore sample (b–3106) taken from the outcrop gave the values 0.14% Cu and 5.38% S. X-ray diffraction the same sample showed potash feldspar, sericite and malachite.

(8) MB–3 Outcrop

The outcrop is an ore vein formed in quartz diorite on the western tributary midstream of the Mamising Creek. The outcrop and its occurrence are shown in Fig. I–6.

The main constituent ore minerals are pyrite, chalcopyrite and malachite. Gangue minerals are quartz and calcite associated with small amount of chlorite. Pyrite and malachite are disseminated in the country rock of quartz diorite.

The analytical results of the channel sample from the center of the outcrop (b–3126) and a lump ore sample of pyrite and malachite dissemination in quartz diorite (b–3127) is as follows:

	Sampling width (m)	Cu %	S %
b–3126	0.15	1.91	1.40
b–3127	(lump)	0.62	0.58

It was shown that the vein was rich in copper mineral though small in width.

X-ray diffractive analysis was made on three samples, B–3126, b–3127 and b–3128 taken from quartz diorite. Chlorite, laumontite and montmorillonite were detected.

The result of analysis of a lump ore sample (b–3117) taken from the fracture zone containing veinlets of chalcopyrite-pyrite-malachite with the bearing of N 5°E and 30°E and the width of 50 cm, gave 8.52% Cu and 7.71% S. It is high in copper grade though it consists of small veinlets.

(9) MB–4 Outcrop

It is a dissemination zone of malachite and azurite located 100 m northwest of MB–3

outcrop. The host rock is quartz diorite strongly silicified, argillized and chloritized. Although the whole width of mineralization is about one meter, the rich part in copper is the center zone with the width of 0.40 ∿ 0.45 m.

The result of analyses of the samples such as a channel sample from the center part (b–3133), lump ore samples containing copper minerals from the same part (b–3130, m–3170) and a malachite bearing lump ore sample taken from the dissemination at the footwall (b–3132), is as follows:

	Sampling width (m)	Cu %	S %	Au g/t	Ag g/t
b–3130	(lump)	4.80	0.07	–	–
b–3132	(lump)	1.75	0.03	–	–
b–3133	0.40	4.81	0.07	0.0	38.8
m-3170	(lump)	2.30	0.14	0.0	4.6

It is judged from these assay that the content of sulfide minerals is very poor. In microscopic observation, copper sulfide mineral was not observed other than secondary copper minerals.

(10) MF–1 Outcrop

The outcrop is situated at the headwaters of the Mabileng Creek, a tributary of the Mamising Creek. It consists of pyrite and chalcopyrite dissemination zone in quartz diorite being exposed discontinuously for about 30 m along the creek. The result of analysis of a lump ore sample in which chalcopyrite seems scattered megascopically (f–3124), showed 1.41% Cu and 3.35% S.

Microscopic observation of the ore sample showed fine veinlets of pyrite and chalcopyrite in the country rock and scattered magnetite grains. Magnetite is euhedral, fine crystals less than 0.3 mm. Pyrite occurs as euhedral-subhedral, coarse crystals and chalcopyrite as irregular fine veinlets. Chalcopyrite veinlets cut magnetite grains. Sometimes, micro-grains of pyrite and chalcopyrite fill the interstices of magnetite grains. Small amount of ilmenite in tiny grains are contained as the primary iron oxide.

These are the descriptions of the main outcrops distributed in the basin of the Mamising Creek. It can not be said, however, that the mutual relation between the outcrops was fully elucidated because of absence of exposure as it is covered by thick vegetation in spaces between the outcrops.

On the other hand, several small scale dissemination of pyrite were found here and there in the area beside the outcrops described above. Therefore, the extent of mineralization

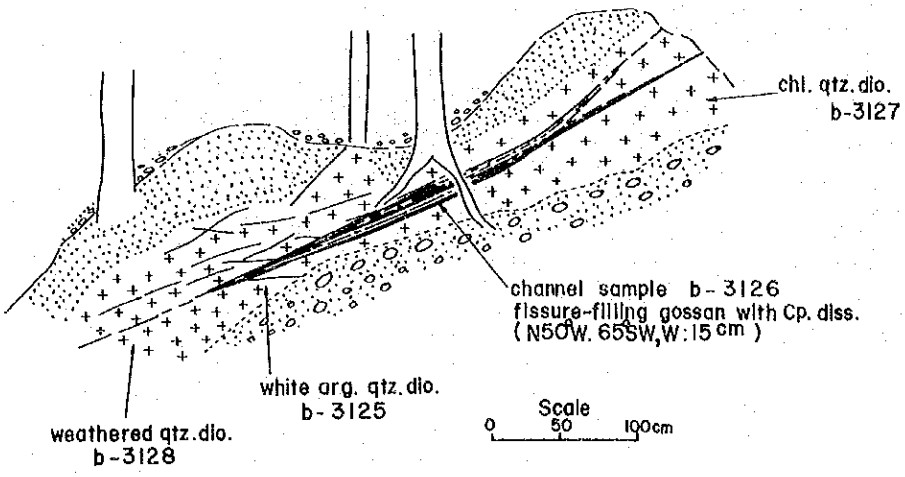

Fig. I–6 Sketch of MB–3 Mineralized Outcrop

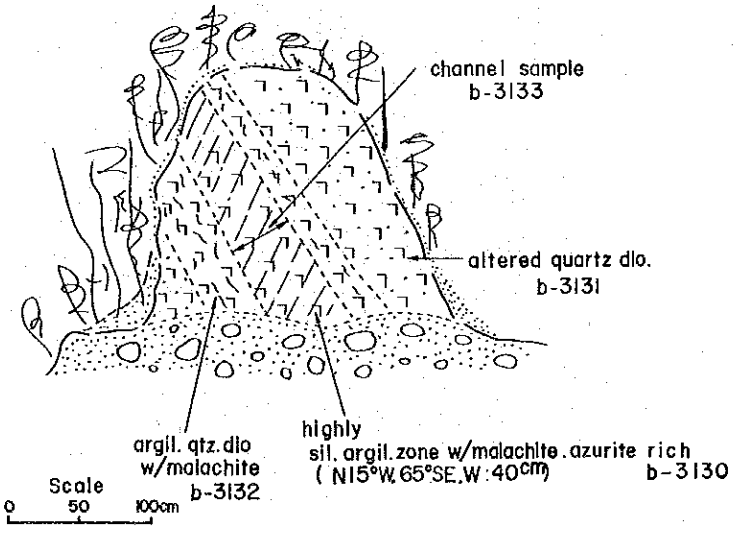

Fig. I–7 Sketch of MB–4 Mineralized Outcrop

might be considered to be 1.2 km x 1.0 km as previously mentioned.

Three drill holes were excavated this year at the eastern margin of the mineralized zone. The result will be described in detail in the next chapter.

3–2–2 Mineralized Subzone on the West of Ud-Udiao

This subzone is situated on the northern bank of the Manikbel River, 700 m to the west of Ud-Udiao, and consists of seven veins of various sizes. These veins can be observed at the entrance and inside the cross-cut (13.7 m long), excavated by Marcopper Mining Corporation in the past. The distribution of veins is shown in Fig. I–8. The country rock is a chloritized porphyritic andesite lava, remarkably silicified near the ore vein.

The seven veins include three pyrite-quartz veins (No. 1, No. 2 and No. 4) and four veinlets of pyrite and calcite (No. 3, No. 5, No. 6 and No. 7). No. 1 vein is the most excellent in scale as well as in grade.

(1) No. 1 Vein

It is a pyrite-chalcopyrite-quartz vein exposed near the entrance of the cross-cut showing a strike of N 70°E and dips 80°N with a maximum width of 80 cm. It is observed as two outcrops at the distance of about 4 m. The outcrop at the eastern side is a stable vein 80 cm in width associated with abundant pyrite and chalcopyrite, while in the western side, the vein is branched off, and the main portion could not be observed because of soil overburden.

The result of analyses of the channel samples from the eastern and western outcrops (a–3101, a–3103) and the lump ore samples of pyrite-chalcopyrite concentration from the eastern outcrop (a–3102 and m–3105), is as follows:

	Sampling width (m)	Cu %	S %	Au g/t	Ag g/t
a–3101	0.80	4.82	5.30	0.2	38.6
a–3102	(lump)	16.39	16.56	2.4	64.4
a–3103	0.20	6.50	7.98	0.5	37.2
m–3105	(lump)	4.48	5.12	0.9	39.1

Microscopic observation of the part rich in chalcopyrite showed that the polished section contains abundant chalcopyrite and magnetite associated with small amount of sphalerite. Chalcopyrite shows dissemination controlled by fine prismatic gangue minerals. Magnetite occurs commonly as grains, sometimes showing irregular form such as filling the cracks of gangue minerals. Sphalerite is observed in small amount as fine grained inclusion in chalcopyrite. It includes very fine grains of chalcopyrite often.

Silver mineral could not be confirmed notwithstanding its high content. It is possibly contained in chalcopyrite as solid solution.

A limonite stained silicified zone with strike of N 30°E, dip of 70°E and width of 0.8 ∿ 1.0 m is found on the northern bank of the Manikbel River about 50 m to the west of the vein. No sulfide ore could be observed even in a small pit excavated in the zone although only small amount of malachite was observed.

A detailed field investigation was made in the surrounding area of vein No. 1 in order to confirm the lateral extension of the vein. No outcrop could be located to correspond to it.

(2) No. 2 Vein

Although the it is a pyrite-quartz vein similar to No. 1, it contains of less sulfide minerals and quartz takes a network form. Chalcopyrite could not be observed megascopically.

The result of analysis of a channel sample (a–3104, 30 cm in vein width) showed 0.26% Cu, 3.79% S, 0.1 g/t Au, and 3.2 g/t Ag, which is inferior in grades.

(3) No. 4 Vein

It is a pyrite-quartz vein located about 7 m from the entrance of the cross-cut, associated with abundant clay. On the eastern wall, the vein width is 25 cm, while on the western wall, pyrite is 5 cm wide, and the main part of the vein consists of quartz and clay zone having total width of 40 cm.

Analysis of a channel sample taken from the eastern wall showed 0.16% Cu and 14.26% S.

(4) No. 3 Vein and No. 5 Vein

Both are small calcite veins less than 5 cm width, scattered with pyrite in No. 3 while barren in No. 5.

(5) No. 6 Vein and No. 7 Vein

These veins are calcite veinlets with 1 ∿ 2 cm width formed in two shear zones having the width of 20 cm and 5 cm, respectively. Very small amount of pyrite is observed in No. 6 vein, while No. 7 vein is quite barren.

A lump ore sample from No. 6 vein (a–3106) gave low analytical values such as 0.03% Cu and 0.23% S. Thus, both veins together with No. 3 and No. 5 vein are not worthy of further exploration.

Among the mineralized zones located west of Ud-Udiao, No. 1 vein is the most interesting target. However, the vein is situated very close to the main stream of the Manikbel

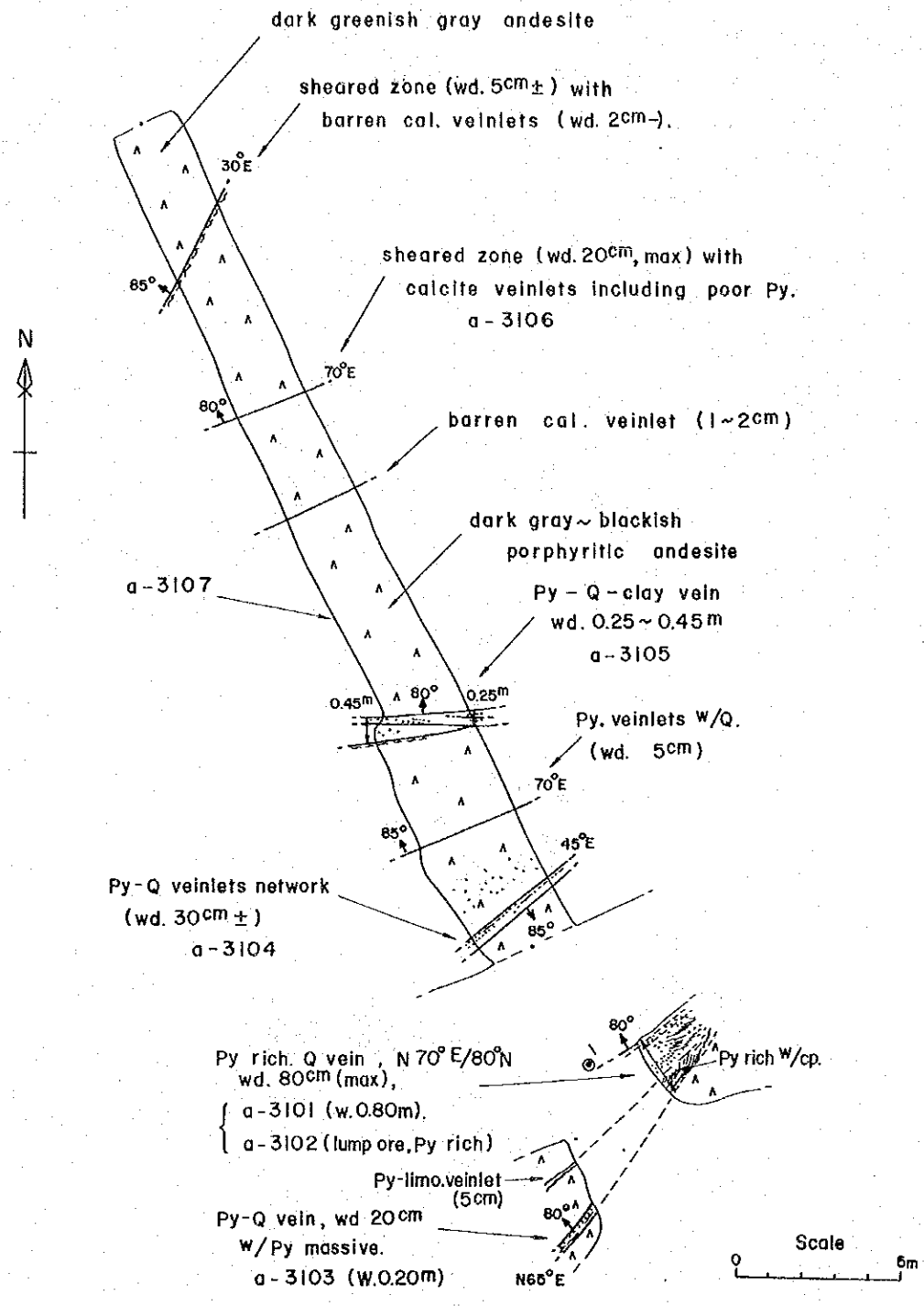

Fig. I–8 Distribution Map of Veins in MA–1 Mineralized Subzone

River, at distance of only 10 m and also extends in a direction parallel to the stream. Therefore, it is considered to be difficult to carry out exploration and development of the vein as viewed from the topographical standpoint.

3–2–3 Mineralized Subzone on the East of Nagasasan

The subzone consists of MB–2 outcrop located on the downstream of the Kulan Creek, 700 m northeast of Barrio Nagasasan and MD–1 outcrop exposed at the mouth of the Malwa Creek, 600 m east of Nagasasan.

(1) MB–2 Outcrop

It is a strongly silicified zone with a width of 20 cm in quartz diorite showing a strike of N 50°W and dips 45°N. Ore minerals are pyrite and malachite. Pyrite is abundantly contained in the strongly silicified zone and also scattered in the surrounding host rock in the form of dissemination. Malachite is observed to have been scattered in the silicified zone. The result of analysis of a massive sample (b–3114) showed 1.32% Cu and 16.97% S showing a little higher grade in copper. However, no copper mineral was observed in the outcrop.

(2) MD–1 Outcrop

The mineralization of the outcrop consists of a pyrite veinlet formed along hanging wall of the shear zone (strike N 80°E, dip 80°N, width 25 cm) in quartz diorite, in which the aggregate of massive pyrite almost without gangue minerals.

Pyrite includes an unidentified black mineral. The result of analysis of the sample of massive pyrite (d–3113) taken from the outcrop showed values of 2.98% Cu, 37.20% S, 0.0 g/t Au and 5.7 g/t Ag.

As described above, both outcrops are vein type mineralization in quartz diorite. The content of copper is at the same level to that of dissemination type mineralization, and yet the vein width is small. Therefore, it does not warrant further exploration.

Other outcrops containing pyrite dissemination-veinlet found in places are all small in scale and contain no primary copper mineral, they are considered to be local mineralization.

3–3 Mineralized Zone in Layacan Area

All the mineralized zones observed in the area are vein type, and are distributed along the main stream of Balasian River and along the Segseg Creek at the southern end of the survey area. Three mineralized zones along the Balasian River are found. One is emplaced in basalt-basic andesite lava of the Licuan Group Formation I and quartz diorite. Two

mineralized zones along the Segseg Creek occurs in the country rocks such as basalt lava of Licuan Group Formation I and dacite lava of Tineg Formation.

Outline of the mineralized zones is shown in Table I–5.

3–3–1 LA–1 Mineralized Subzone along Balasian River

The mineralized zone is situated on the northern bank of the Balasian River, and consists of white clay vein in altered basic andesite and three pyrite-clay veins in the country rock of quartz diorite. Both host rocks are strongly silicified and argillization is often observed along the contacts with the vein. The locality of each vein is shown in Fig. I–10.

The outline of the veins are as follows:

(1) No. 1 Vein

It is a white clay vein in andesite, and only small amount of pyrite is contained. The result of analysis (a–3349) showed nil amount of gold and silver minerals although the occurrence of them was expected. As a result of X-ray diffractive analysis chlorite, sericite and abundant amount of montmorillonite were detected, which leads to the assumption that the main constituent minerals of the clay are silica, sericite and montmorillonite.

(2) No. 2 Vein

The vein is a clayey vein with a width of 15 ∿ 20 cm containing abundant pyrite, associated with very small amount of quartz as gangue mineral. No ore mineral other than pyrite was observed by the naked eye, and the result of analysis (a–3350) showed gold value of 12.2 g/t with no copper content. The clay consists sericite.

(3) No. 3 Vein

The vein is a strongly silicified zone with a width of 1.50 m associated with white clay. The result of X-ray diffraction showed the clay was mainly composed of chlorite, sericite and kaolinite. Pyrite is relatively coarse grained and often shows euhedral crystal form.

The result of analysis of a channel sample (a–3351) showed higher grade of silver, 18.3 g/t with no copper content.

(4) No. 4 Vein

It is a clay vein containing abundant pyrite 60 cm in width. Pyrite is coarse grained similar to No. 3 vein.

Pyrite is the main constituent mineral of the veins in LA–1 mineralized subzone containing few copper minerals associated with a small amount of gold and silver. A preponderant amount of clay is contained in the veins as gangue mineral, which consists mainly of chlorite and sericite, associated with, dependent on veins, montmorillonite and kaoline.

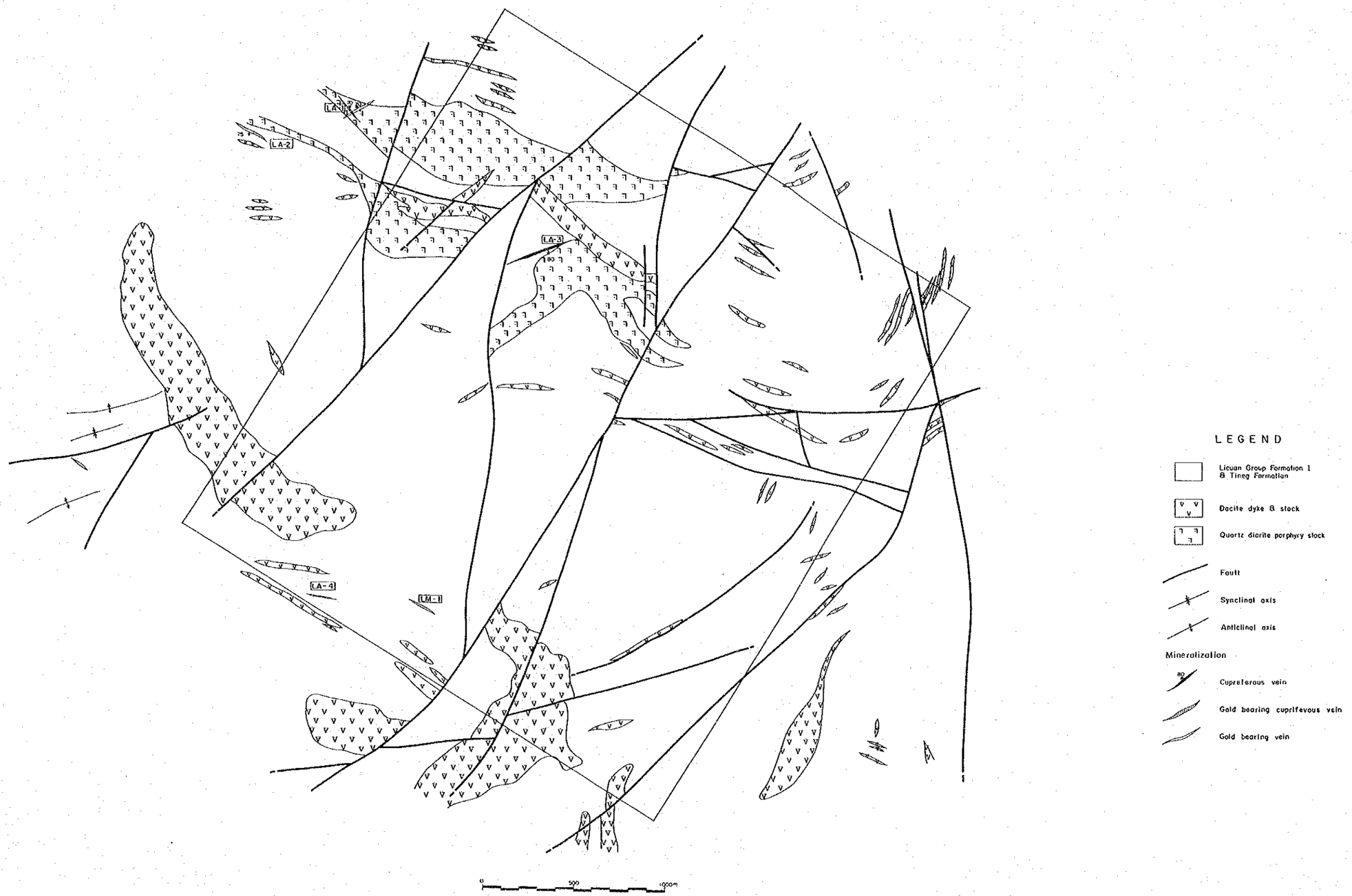

Fig. I–9 Distribution Map of Mineralized Zones in Layacan Area

Table I–5 Summary of Mineralized Zones in Layacan Area

No.	Outcrop No.	Location	Type	Outcrop Scale or Vein Width	Ore Minerals	Gangue or Alteration Minerals	Host Rock	Collected Sample No.	Analytical Results							Occurrence
									Sample No.	V.W	Au	Ag	Cu	Pb	Zn	
1	LA–1	By the Balasian River in the western end of the Layacan area.	Vein	4 veins along Balasian River	Pyrite	Quartz, Sericite Alunite, Kaolinite	Quartz diorite porphyry	a–3350 a–3351	a–3350 a–3351	–m 1.50	12.2g/t 1.3	5.6g/t 18.3	0.01% 0.01	–% –	–% –	This outcrop is composed of 4 pyrite-clay veins striking N40°W ~ N50°W, dipping 70° ~ 85°N. These veins contain abundant pyrite, but no Cu minerals are found. One vein shows high grade of Au.
2	LA–2	About five hundred meters east of LA–1.	Vein	6 veins along Balasian River	Pyrite	Quartz, Kaolinite Sericite, Chlorite	Andesite	a–3343 a–3344 a–3345 a–3346	a–3343 a–3345	2.00 –	0.1 0.2	0.2 0.9	0.05 0.21	– – –	– – –	This outcrop consists of 6 veins within 150 m along the Balasian River. These veins are composed of abundant pyrite and clay, but no Cu minerals are found in all of veins. Gold and Silver are also absent.
3	LA–3	By the lowermost stream of the Kawayen Creek.	Vein	5 veins along Kawayen Cr.	Pyrite, Bornite, Chalcopyrite	Quartz, Pyrophyllite, Diaspor, Sericite	Andesite	a–3353, a–3354, a–3355, a–3356	a–3353 a–3354 a–3355 a–3356	1.30 0.20 – 0.50	0.1 0.5 0.4 0.0	6.4 41.4 11.6 0.8	0.04 25.25 26.01 0.20	– 0.01 0.01 0.00	– 0.04 0.07 0.00	This outcrop is composed of 5 veins containing remarkable pyrite. One vein contains high grade streak of pyrite, bornite and chalcopyrite with azurite and malachite. This vein is the most interesting one in this area.
4	LA–4	By the upper stream of the Segseg Creek.	Vein	10m x 10m	Pyrite, Chalcopyrite Geothite, Sphalerite, Magnetite	Quartz, Kaolinite, Pyrophyllite, Diaspor	Basalt	a–3380 a–3381	a–3380 a–3381	– –	0.2 16.0	0.4 7.1	– 14.64	– –	– –	There are some mining tunnels and many old mine openings in the upper stream of the Segseg Creek. There are only some clay veins observed in the tunnels that are accessible. One sample (a–3380) collected from one ore damp in front of the old mine openning and shows copper content of 16.64.
5	LM–1	About six hundred meters east of LA–4	Vein	V.W. : 0.70m	Pyrite, Malachite	Quartz, Sericite, chlorite	Dacite	m–3361	m–3361	–	0.9	1.3	2.18	–	–	This outcrop is composed of clay vein with malachite stain striking N 62° E in white altered tuff.

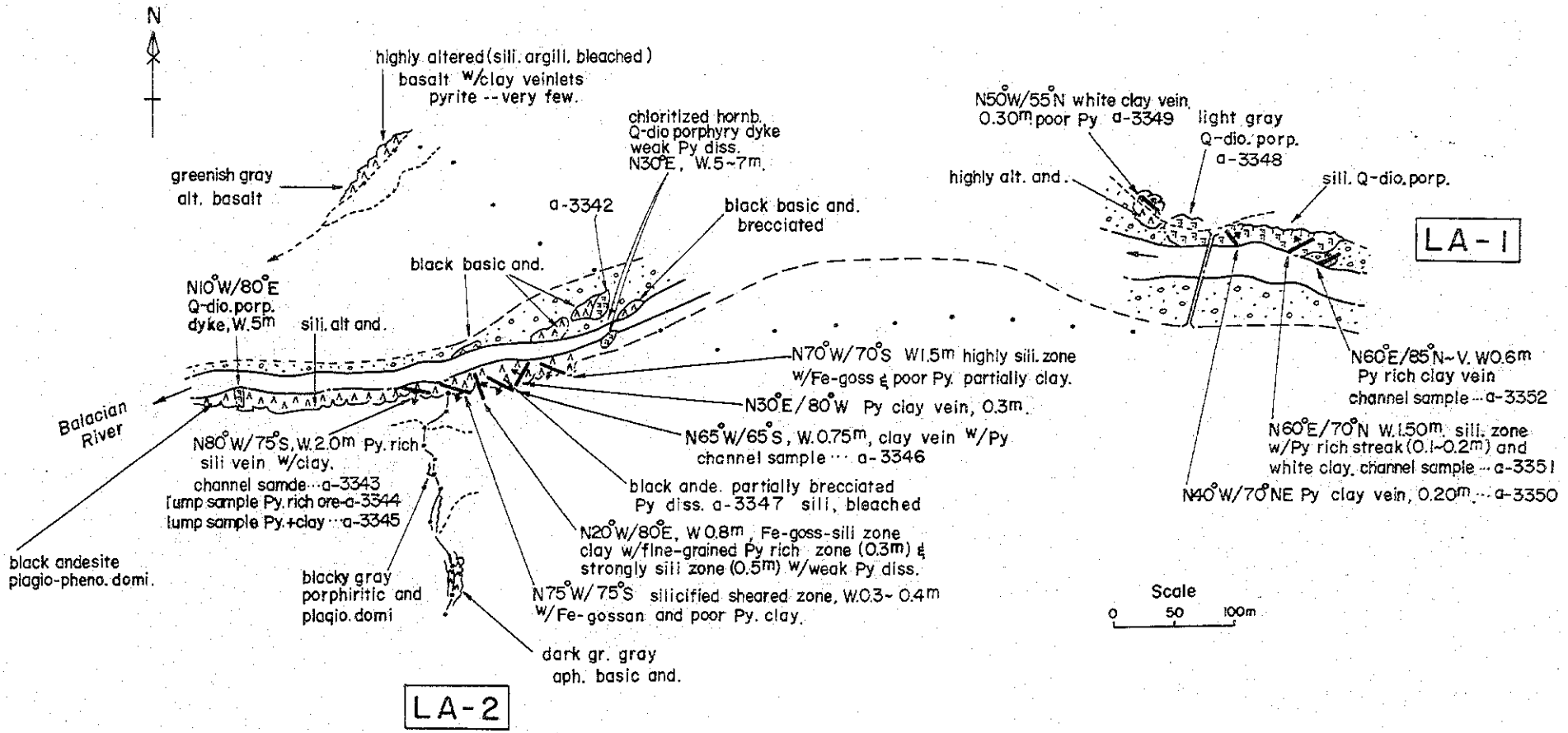

Fig. I–10 Distribution Map of Veins in LA–1 and LA–2 Mineralized Subzones

The result of analysis of the samples taken from the veins are as follows:

Veins	No.	Sampling width (m)	Au g/t	Ag g/t	Cu %
No. 1	a-3349	0.30	0.1	0.6	–
No. 2	a–3350	0.20	12.2	5.6	0.01
No. 3	a–3351	1.50	1.3	18.3	0.01
No. 4	a–3352	0.60	0.0	0.1	0.01

3–3–2 LA–2 Mineralized Subzone along Balasian River

As shown in Fig.I–10, the mineralized zone is located on the southern bank of the Balasian River about 500 m downstresm from LA–1 mineralized subzone, consisting of six veins formed within the chloritized basic andesite.

(1) No. 1 Vein

It is a strongly silicified zone 2.0 m in width showing strike of N 80°W and dip of 75° S. It contains abundant pyrite and small amount of clay. Pyrite is concentrated in two parts of the vein such as the portion in the hanging wall side, 40 cm in width, and the center part, 60 ∿ 70 cm in width. Pyrite is fine grained. The result of analyses of a chennel sample (a–3343), a lump sample of silicified part rich in pyrite (a–3344) and a clay sample abundant in pyrite (a–3345), showed the copper grade as low as 0.01 ∿ 0.21%, and gold and silver were almost absent.

From X-ray diffractive analysis of the three samples, sericite was not detected at all, and abundant alunite and a small amount of kaolinite were detected instead.

(2) No. 2 Vein and No. 6 Vein

Both veins show similar character. The veins are strongly silicified zones poor in pyrite associated with clay, with remarkable limonite contamination. Pyrite occurs throughout the silicified zones in disseminated form.

(3) No. 3 Vein and No. 5 Vein

These are limonite clay veins containing abundant pyrite similar to No. 1. No. 3 vein has a massive pyrite with width of 30 cm from the vein width of 80 cm. Notwithstanding that these are the veins rich in sulfide mineral, copper mineral could not be observed at all.

(4) No. 4 Vein

The mineralization of the vein is a thick dissemination of fine grained pyrite in clayey part, grayish white to white in color, consisting mainly of pyrite. The result of analysis of a channel sample (a–3346) showed almost nil content of gold and silver as well as copper.

The clay of the vein contains abundant chlorite and sericite.

Assay values of copper, gold and silver of the samples taken from No. 1 and No. 4 veins are as follows:

Veins	Sample No.	Sampling width (m)	Cu %	Au g/t	Ag g/t
No. 1	a–3343	2.00	0.05	0.1	0.2
No. 1	a–3344	(lamp)	0.01	0.0	0.1
No. 1	a–3345	(lamp)	0.21	0.2	0.9
No. 4	a–3346	0.70	0.01	0.0	0.3

3–3–3 LA–3 Mineralized Subzone along Balasian River

The mineralized zone is situated the downstream of the Kawayen Creek, a tributary of the Balasian River, and consists of five veins of various sizes shown in Fig. I–11. The veins are emplaced in the host rock of highly altered basic andesite. It is concentrated near the boundary with quartz diorite porphyry stock in the surrounding area.

The occurrence and grade of the veins are described in the following.

(1) No. 1 Vein

The vein is a pyrite-clay vein with 1.10 m in width showing strike of N 70°E and dip of 70°N, associated with very small amount of secondary malachite. Pyrite is concentrated in the foot-wall side of the vein with width of 65 cm. The vein width is 1.10 m. Malachite was formed on the surface coating pyrite concentration, in which copper sulfide is not observed.

The result of analysis of a channel sample (a–3317, 65 cm in width) from pyrite concentration showed 0.03% Cu, 0.0 g/t Au and 0.4 g/t Ag.

As the result of X-ray diffractive analysis of the clay in the vein of hanging wall, abundant pyrophyllite as well as sericite were detected.

(2) No. 2 Vein

It is a pyrite-clay vein 2.0 m in width formed in highly silicified and argillized andesite associated with two streaks of bornite- chalcopyrite-pyrite with the width of 20 cm and 1–2 cm respectively. This is the single vein containing copper sulfide from the mineralized zones along the Balasian River.

Malachite and azurite were formed on the surface of the copper bearing streaks. The vein consist, as shown in Fig. I–11, from the hanging wall to foot wall, of (i) pyrite and clay, 1.30 m in width (a–3353), (ii) high grade streak of bornite-chalcopyrite-pyrite, 20 cm in width (a–3354, a–3355) and (iii) silicified argillaceous part with pyrite dissemination,

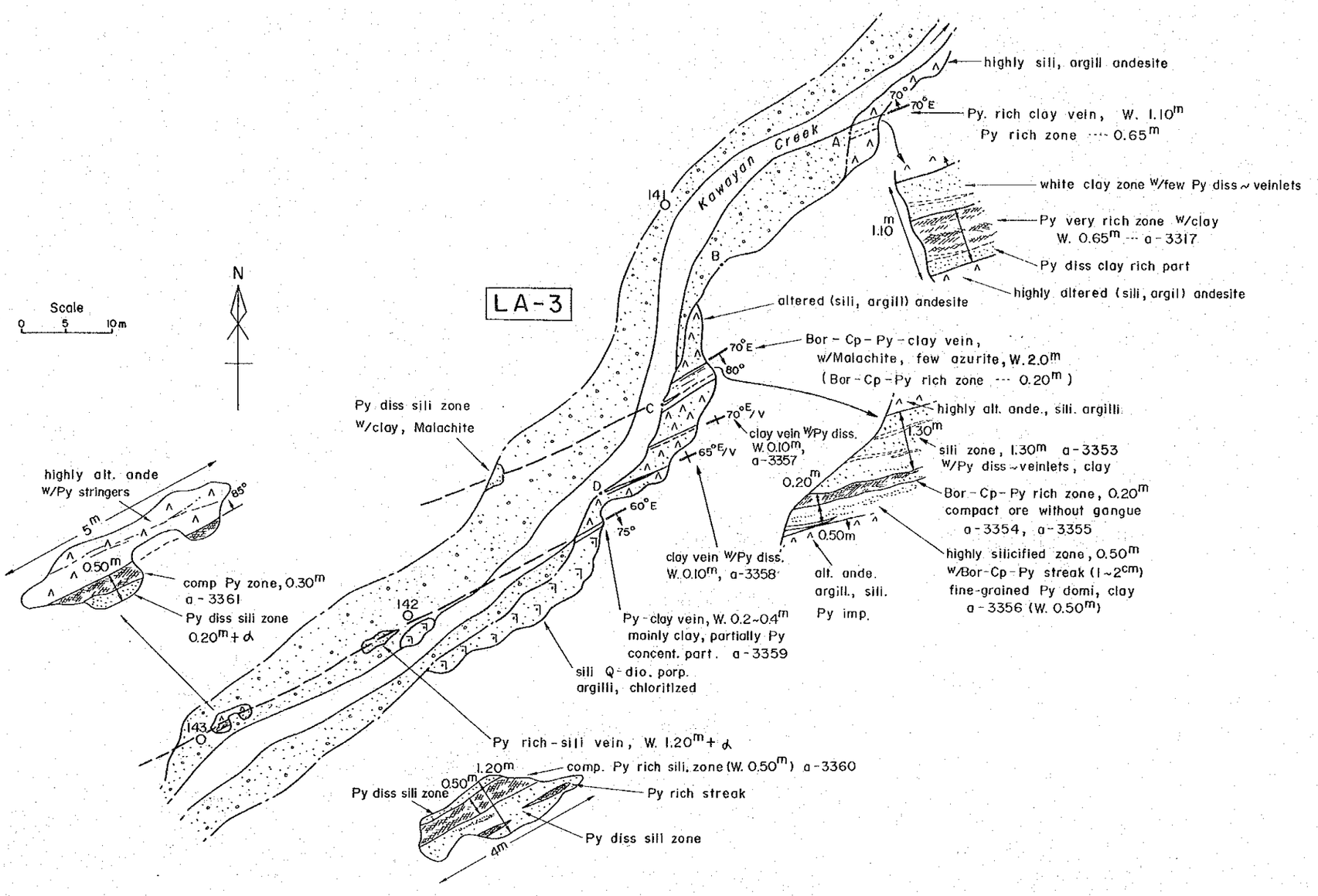

Fig. I–11 Distribution Map of Veins in LA–3 Mineralized Subzone

50 cm in width, associated with a streak (1–2 cm) of bornite and chalcopyrite (a–3356).

The result of analysis of each portion is as follows:

	Sampling width (m)	Au g/t	Ag g/t	Cu %	Pb %	Zn %
a–3353	1.30	0.1	6.4	0.04	–	–
a–3354	0.20	0.5	41.4	25.25	0.01	0.04
a–3355	(lump)	0.4	11.6	26.01	0.01	0.07
a–3356	0.50	0.0	0.8	0.20	0.00	0.00

Microscopic observation of sample a–3355 showed that chalcopyrite altered to secondary copper sulfide such as bornite and digenite although it was originally formed as primary mineral and that chalcopyrite could be observed in small amount only as a relic mineral after replacement. Pyrite occurred as an aggregate of fine to medium-grained crystals, interstices of which were filled by bornite and digenite.

Abundant amount of pyrophyllite and diaspore were detected from the clay of samples a–3353 and a–3356, but sericite was not detected.

On the opposite bank of the outcrop, a small outcrop in a silicified zone with pyrite dissemination covered with secondary malachite is found which is considered to correspond to the extension of No. 2 vein relative to its position and the condition of malachite formation.

(3) No. 3 Vein and No. 4 Vein

Both are clay veins having width of 10 cm each, associated with dissemination or veinlets of pyrite. No copper mineral can be observed. Assays for gold and silver of the samples from No. 3 (a–3357) and No. 4 vein (a–3358) showed no values for both elements.

(4) No. 5 Vein

It is a pyrite-clay vein formed along the boundary between altered andesite and quartz diorite porphyry stock, and is observed as three discontinuous outcrops exposed from the eastern bank of the Kawayen Creek to the western bank.

The outcrop on the eastern bank consists mainly of clay having a width of 20–40 cm (a–3359). The outcrop in the middle of the creek has a vein width of 1.20 m associated with pyrite concentration 50 cm wide (a–3360). On the surface of outcrop on the western bank, pyrite concentration with width of 30 cm (a–3361) is observed although the detail could not be known because of small outcrop extent.

The grades of the three outcrops are as follows:

	Sampling width (m)	Au g/t	Ag g/t	Cu %
a–3359	0.30	0.3	3.6	0.29
a–3360	0.50	0.0	4.2	0.24
a–3361	0.30	0.0	1.4	0.06

As described above, LA–3 mineralized subzone is characterized by the occurrence of veins containing abundant sulfide. However, No. 2 vein is the only vein which contains copper sulfide minerals, while other veins consist mainly of pyrite as the sulfide mineral, and, in addition, the grades of gold and silver are lower than those of LA–1 mineralized subzone.

3–3–4 Mineralized Subzone along Segseg Creek

The subzone consists of LA–4 outcrop and LM–1 outcrop located in the upstream of the Segseg Creek in the southern part of the survey area. The former is an irregular vein in basalt lava and the latter is a vein in dacite lava.

(1) LA–4 Outcrop

It is an irregular quartz network zone exposed on the northern bank in the upstream of the Segseg Creek. The host rock was altered to soft, white rock by strong silicification and argillization.

At the outcrop, any sulfide minerals could not be observed other than pyrite. However, unsystematic stopping has been done within the extent of 10 m x 10 m. Mining and planning are being continued in small scale as a home business by local peoples.

The result of analysis of the silicified zone containing quartz veinlets (a–3380) showed low values of gold and silver.

At the present underground working face, small veins and lenses containing pyrite and small amount of chalcopyrite and covellite are excavated from a strongly silicified rock, which are stored on the surface near the entrance of the adit.

The result of analysis of a lump ore sample (a–3381) rich in pyrite and covellite taken from the ore dump showed content of gold though small in amount.

The result of analysis of the above ore and the sample from the white silicified rock is as follows:

		Au g/t	Ag g/t	Cu %
a–3380	White silicified quartzy rock	0.2	0.4	–
a–3381	Pyrite and covellite	16.0	7.1	14.64

As a result of X-ray diffractive analysis pyrophyllite, diaspore and kaolinite were detected from a–3380, and goethite, chalcopyrite and sphalerite from a–3381, both in very small amount.

From microscopic observation results, the sample was shown to be porous, and contains an aggregate of medium- to fine-grained pyrite and a lamella aggregate of covellite crystallized in the cavity was observed. Chalcopyrite could not be observed in the polished section.

(2) LM–1 Outcrop

The outcrop is a clay vein located about 600 m east of LA–4 where a small scale irregular stoping is carried out for gold and silver in soft clayey part.

The vein is a highly argillized zone in silicified and argillized dacite, in which disseminated malachite is the only ore mineral observed. Although the highly silicified zone is 70 cm in width, the surrounding part underwent remarkable argillization. The main clay mineral is sericite.

A lump sample taken from the stoping face (m–3361) showed the values of 2.18% Cu, 0.9 g/t Au and 1.3 g/t Ag. Although the grade of copper might be workable, those of gold and silver which were the object of mining, are quite low.

Distribution and conditions of the main mineralized zones in the Layacan area are as described above. However, some other manifestation have been confirmed beside the mineralized zones and outcrops mentioned above. A number of pyrite-quartz or clay veinlets are found at the confluence of the Adawey Creek with the Balasian River, in a part of which unsystematic stoping is being carried out for gold and silver. The veins are, however, small in scale having narrow width, and the result of analysis of the samples taken form the main veins, showed low values for gold, silver and copper.

It will be concluded, therefore, that the mineralization does not appear to have high potential for exploration.

Although several small scale traces of mining are found along the ridge from Barrio Patiacan to Mt. Quinali and in the Segseg Creek basin they are the traces of old mining in

highly silicified and argillized zones in silicified dacite, where quartz vein was hardly observed. The result of assay of several samples did not show high values. From these, it is difficult to expect a large scale deposit for gold and silver.

Further, in the Layacan area, any outcrop of dissemination-network considered, the porphyry copper type deposit has not been confirmed at all, showing a remarkable contrast with the Manikbel area.

PART II GEOCHEMICAL SURVEY

1. GENERAL REMARKS

In this project area, the reconnaissance and semi-detailed geochemical surveys for stream sediments had been conducted previously in Phase I and II, respectively, to delineate mineralized zones from the whole project area. Detailed geochemical soil sampling had also been undertaken to select promising area for mineral resources. Results from these surveys were used as an effective criterion for selecting more encouraging areas.

In this phase of the survey, the geochemical soil survey was conducted to determine the extent and intensity of the mineralized zone in the Manikbel and Layacan areas where they were delineated as the most promising area for ore deposits from the second phase survey.

The geochemical soil sampling was considered to cover entirely the distribution areas of mineralized and geochemical anomalous zones which were determined earlier from the result of the Phase I and II surveys. Soil samples of 191 pieces taken from the Manikbel area were analyzed for Cu in BMG, Manila, and 320 samples collected from the Layacan area were analyzed in Japan.

Analytical data of both areas were separately treated statistically and interpreted together with other survey results.

The following description is the details of the geochemical survey for soil carried out in this phase.

2. OUTLINE OF GEOCHEMICAL SURVEY

2–1 Sampling and Analysis

The soil samples were collected along the geological survey routes previously planned to cover entirely the mineralized zones and the geochemical anomalous zones detected by the second phase survey.

In the Manikbel area, the systematic grid-sampling was particularly done along the IP electric survey lines to discuss on the relationship between geochemical and IP electric survey results.

The geochemical soil sampling in the Layacan area was not undertaken in Phase I and II, therefore, the survey routes and sampling intervals were planned so as to cover a greater area and as equally spaced sample location as possible. The average sampling density in the Manikbel area is 60 pieces/sq.km and 32 pieces/sq.km in the Layacan area.

Each soil sample is taken from the accumulated zone (B horizon) and placed in vinyl bags for delivery to the base camp. After drying, each sample is screened to 80 mesh for analysis. All samples collected in the Manikbel area were sent to Manila and analyzed for Cu by BMG. On the other hand, each of the 320 samples taken from the Layacan area were divided into two parts; one part for BMG, and the other half was brought to Japan to be analyzed by the same method as BMG.

All collected samples were analyzed quantitatively for Cu by the atomic absorption method.

2–2 Treatment of Analytical Data

The analytical data of the 191 soil samples in the Manikbel area and 320 samples in the Layacan area were individually treated to determine the geochemical anomalous zones by adopting the simplified statistical treatment method of Lepeltier (1969). Fig. II–1 shows the cumulative frequency distribution of Cu in both the areas.

From these two diagrams, the following statistical values were obtained.

	b	ip	b + s	b + 2s
Manikbel Area	265 ppm	300 ppm	800 ppm	2,650 ppm
Layacan Area	105	225	225	900

b : Mean background value
ip : Abscissa of inflection point
s : Standard deviation
b + s : Value read from abscissa of 16% probability
b + 2s : Value read from abscissa of 2.5% probability

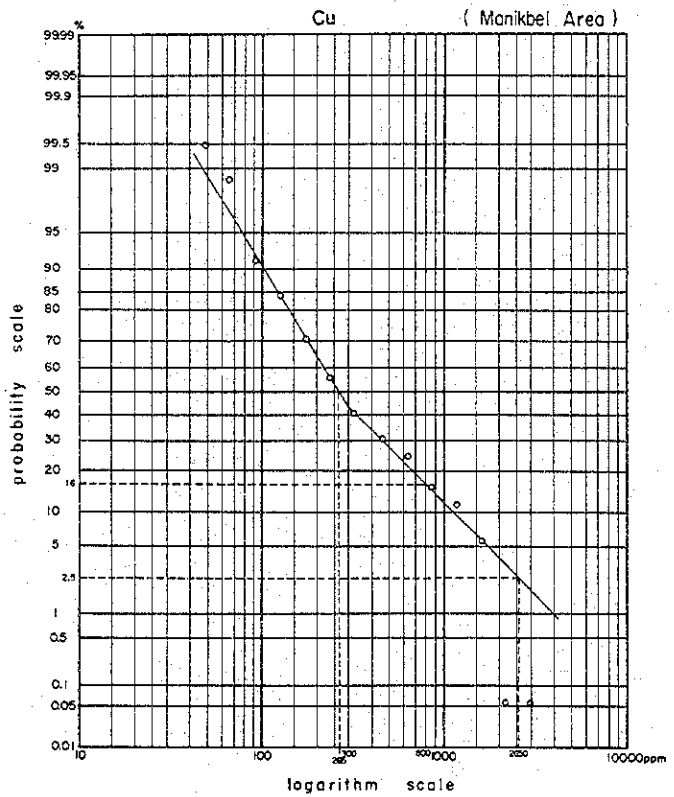

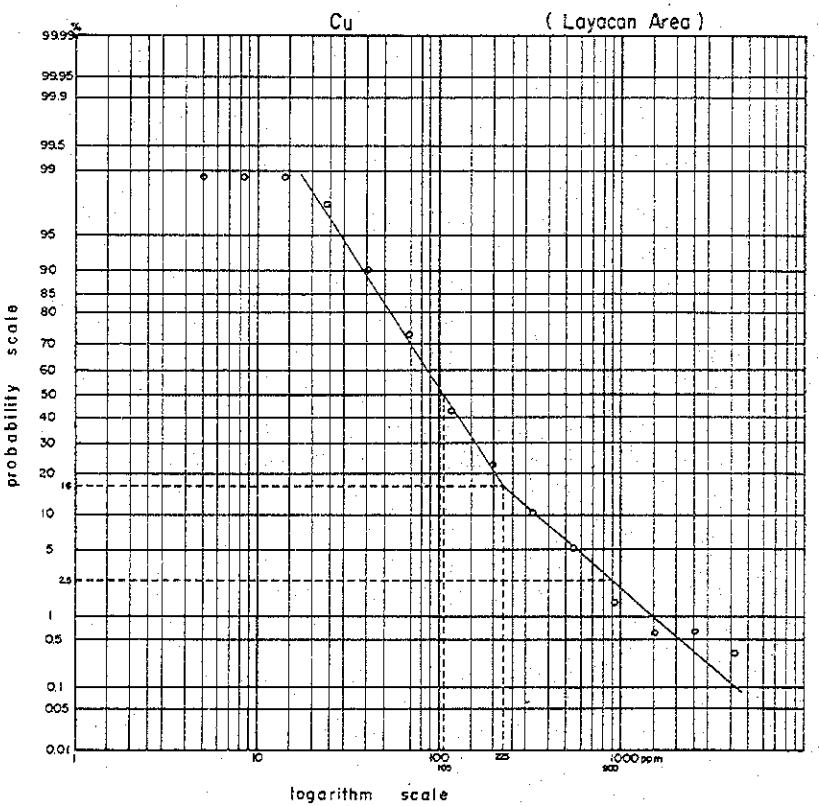

Fig. II–1 Cumulative Frequency Distribution Diagram of Cu in Manikbel and Layacan Areas

Generally, the threshold value (t) can be obtained from abscissa of 2.5%-probability (b + 2s), but if the winding line is obtained on the graph, the threshold value can be shown as abscissa of winding point. In case of this phase survey, the winding point values of both areas are very low so that the threshold values were read as abscissas of 2.5%-probability and abscissas of winding point were used as subsidiary threshold values to draw the distribution map of geochemical anomalies.

PL. II–1–1 and PL. II–2–1 show the distribution of geochemical anomalous zones in the Manikbel and Layacan areas, respectively. These maps were made by using the following rounded values.

	b	t″	t′	t
Manikbel Area	– ppm	300 ppm	800 ppm	2,500 ppm
Layacan Area	100	–	200	900

b : Mean background value

t″ and t′ : Subsidiary threshold values

t : Threshold value

3. DISTRIBUTION OF GEOCHEMICAL ANOMALOUS ZONES

3–1 Manikbel Area

It has been revealed by the second phase geological and geochemical surveys that numerous mineralized outcrops and geochemical anomalous zones are distributed along the Mamising Creek in this area as shown in Fig. II–2. The detailed geochemical survey of this phase was mainly conducted in the Mamising Creek basin and along the IP survey lines. As the result of this investigation, the remarkable Cu anomalous zone covering an area of 1.5 km E-W direction and 1.0 km N-S direction was detected along the Mamising Creek. This zone can be divided into two parts, western and eastern, bounded by the said creek.

The western anomalous zone consists mainly of anomalous points of less than 800 ppm Cu with only three points showing more than 800 ppm Cu. This anomalous zone is located in the distribution area of quartz diorite, and covers the dissemination and vein type mineralized outcrops.

The eastern anomalous zone is distributed on the divide between the Mamising Creek and the Manikbel River and its western side, and it is a higher anomalous zone emphasized by three anomalies points of over 2,500 ppm Cu. This zone spreads over the contact between quartz diorite and andesite lava of the Licuan Group Formation II, particularly the stock of granodiorite intruded into the quartz diorite mass near the contact. The highest anomalous part, over the threshold value (2,500 ppm), of this zone extends along the boundary of quartz diorite and andesite lava with the MA-2, MA-3 and MA-4 mineralized outcrops exposed within this highest anomalous part. It is obvious, therefore, the distribution feature of geochemical anomalous zone is consistent with that of the mineralized outcrops.

In the eastern portion of this anomalous zone, especially the eastern side of the Line-H of the IP electric survey, no mineralized outcrops accompanied by geochemical anomalous zones were found and it is in excellent contrast with the Mamising Creek basin where the remarkable mineralized outcrops are distributed with the widely spread geochemical anomalous zone. This striking contrast seems to be caused by the intrusion of granodiorite.

As previously stated, the granodiorite occurs as the stock intruding into the marginal part of the quartz diorite mass with the same direction of the boundary between quartz diorite and andesite. The mineralization is restrictedly observed in the granodiorite stock and its peripheral portion, particularly in the part of quartz diorite between the granodiorite

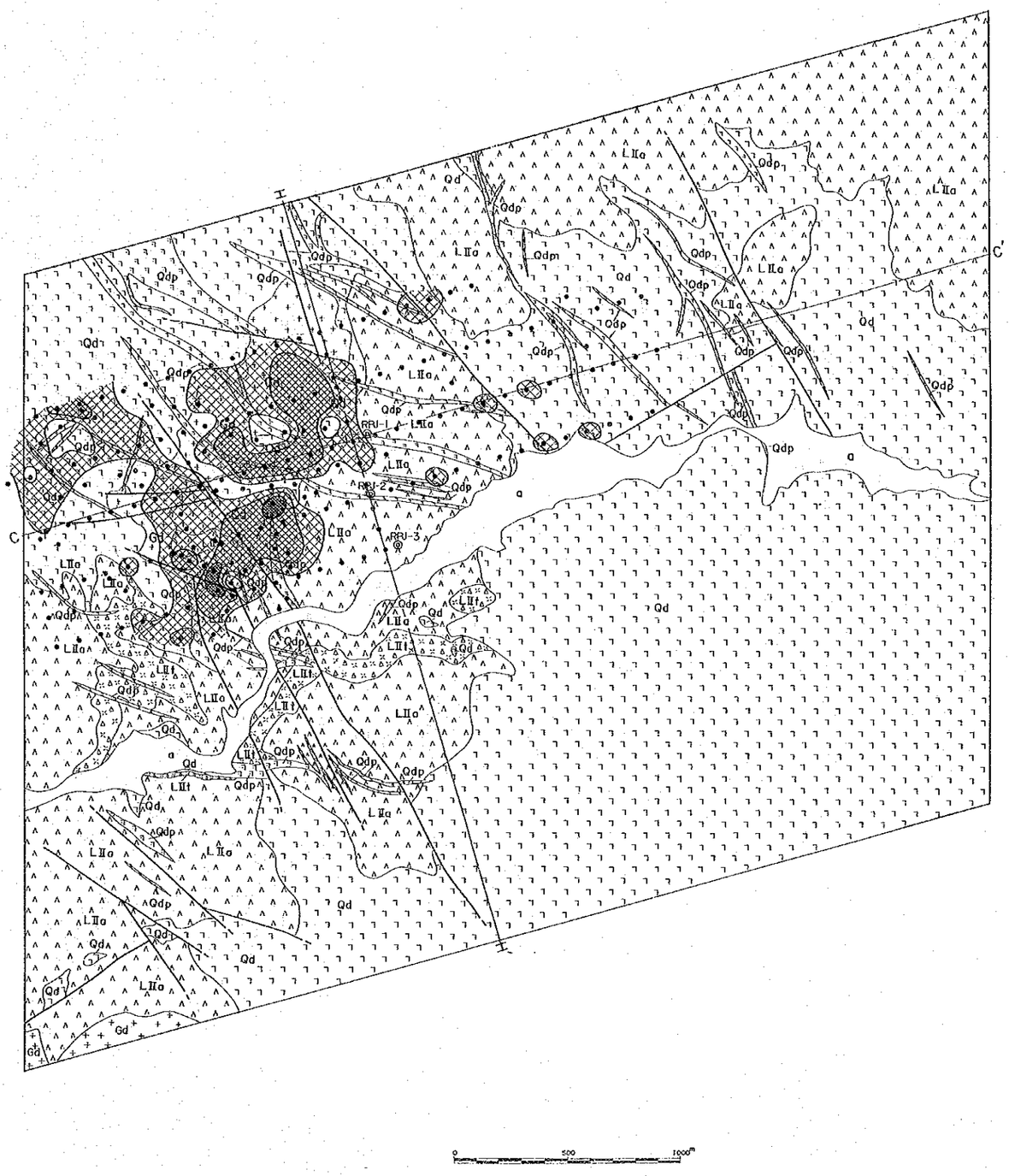

LEGEND

Cu content in soil sample

- ≥ 1 (≧ 2500 ppm)
- 1'~ 1 (800 ppm ~ 2499 ppm)
- 1"~ 1' (300 ppm ~ 799 ppm)

• Sample location

Alluvium
- a — Gravel & sand

Lisuan Group Formation II
- LIIa — Predominant andesite lava
- LIIt — Predominant andesitic pyroclastics

Intrusives
- Qdp — Quartz diorite porphyry ~ dacite dyke
- Gd — Granodiorite
- Qd — Quartz diorite

Others
- Fault
- 70 / 15 — Bedding plane (strike & dip)
- ◎ RPJ-1~3 Drilling site

Fig. II–2 Distribution Map of Geochemical Anomalies in Manikbel Area

stock and andesite lave. In the eastern portion of the Line-H, however, granodiorite stocks are not exposed, and no mineralized zone and no geochemical anomalies are recognized in that portion. From these results of the geological and geochemical surveys, it can be said that the mineralization is closely related to the intrusion of the stock-shaped granodiorite.

3–2 Layacan Area

In the Layacan area, the widely extended geochemical anomalous zone is shown in Fig. II–3. It covers almost one half of the survey area. However, the subsidiary threshold value of this area, which is the lower limit of anomaly, is 200 ppm Cu and it is obviously low in comparison with the subsidiary threshold value of 800 ppm Cu, in the Manikbel area. The lower anomaly range (300 ~ 799 ppm Cu) of the Manikbel area is considered to be equivalent to the intermediate range (200 ~ 899 ppm Cu) of the Layacan area.

From the viewpoint of the above-mentioned fact, the wide anomalous zone can be divided into two zones. One is distributed in the area from Babasig to the southern bank of the Balasian River, and the other from Patiacan to the Balasian River via western portion of Babasig. Besides a few isolated anomalous zones are also found around Pangwew, in the middle to upper streams of the Segseg Creek and other places.

The geochemical anomalous zone distributed from Babasig to the Balasian River contains two points of over 900 ppm Cu and it is the widest zone in this survey area. This anomalous zone overlies the basalt to basic andesite lavas of the Licuan Group Formation I and quartz diorite porphyry intruding the lavas. The extension of this zone is clearly consistent with the exposure of the quartz diorite porphyry. The LA-3 mineralized zone, including a vein consisting of abundant copper minerals, occurs in the central portion of this anomalous zone. At the place equivalent to the extension of that mineralized zone, one anomaly point of more than 900 ppm Cu is situated as showing the notable correlation between the mineralization and the geochemical anomaly.

The anomalous zone extending N-S in the western portion of Babasig is weaker than the above-described zone with the northern half covering the exposures of basalt to basic andesite lavas. The southern half overlies the dacitic pyroclastic rocks of the Tineg Formation. No mineralized zones are recognized within this anomalous zone.

The LA-1 and LA-2 mineralized zones consisting of clay veins with abundant pyrite are located along the Balasian River near the northern end of the western anomalous zone. However, no geochemical anomalies were detected around these mineralized zones. This suggests the absence or lack of copper minerals in both mineralized zones.

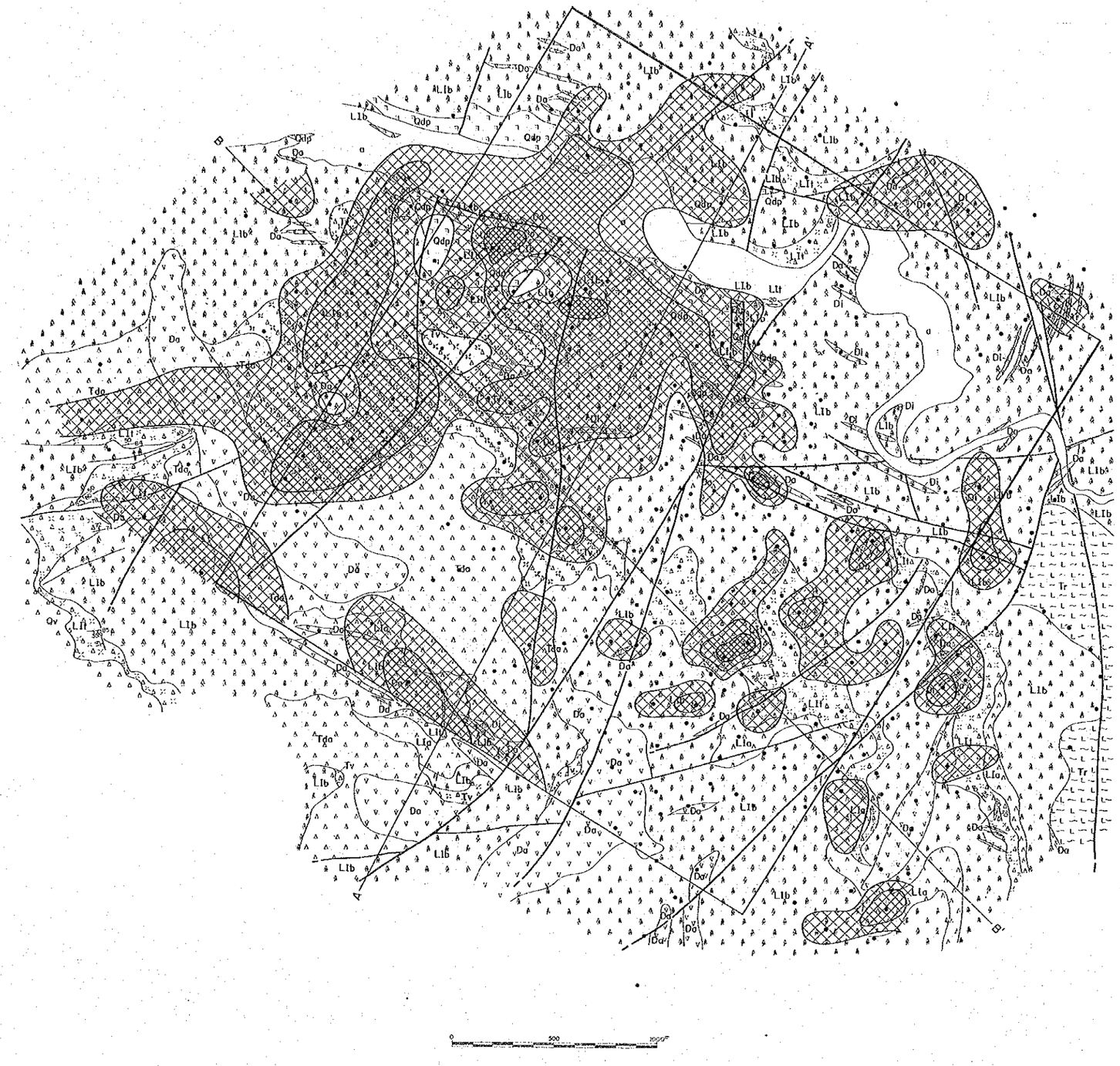

LEGEND

Cu content in soil sample

- ≧1 (≧900ppm)
- 1'~1 (200ppm ~ 899ppm)
- 1"~1' (100ppm ~ 199ppm)

Sample location

- Alluvium — a — Gravel & sand
- Quaternary Volcanics — Qv — Dacitic to andesitic pyroclastics & lava
- Tineg Formation
  - Tda — Dacite lava
  - Tv — Dacitic pyroclastics
  - fr — Rhyolite
- Lleyan Group Formation
  - Llb — Basalt ~ basic andesite lava
  - Lla — Porphyritic andesite lava
  - Llt — Andesitic pyroclastics
- Intrusives
  - Da — Dacite dyke
  - Qdp — Quartz diorite porphyry dyke & stock
  - Di — Micro-diorite ~ dolerite dyke
- Others
  - 20 60 — Bedding plane (strike & dip)
  - Fault
  - Synclinal axis
  - Anticlinal axis
  - A A' — Profile line

Fig. II–3 Distribution Map of Geochemical Anomalies in Layacan Area

Around the southern boundary of the Layacan area, isolated narrow anomalous zones are detected, and the LA-4 and LM-1 mineralized outcrops are located near the anomalous zones. The LA-4 outcrop consists mainly of clay veins with a rare amount of sulfide minerals. The LM-1 outcrop contains secondary copper minerals, therefore, some remarkable geochemical Cu anomalies are expected to occur but no anomalies were detected around the LM-1 outcrop.

Some narrow but intense Cu anomalous zones are distributed in the northern and southern portions of Pangwew, but in these anomalous zones there are no mineralized zone and they are considered to be extremely local.

4. SUMMARY OF SURVEY RESULTS

The main objective of the detailed geochemical soil investigation in this phase survey is to confirm the extension of the mineralized zones with higher accuracy. To achieve this objective, the sampling density of this phase survey was increased from 3.7 pieces per square kilometer of the second phase to 20.4 pieces per square kilometer.

As the result of the detailed investigation, the remarkable Cu anomalous zone is obtained in the Manikbel area. This anomalous zone is nearly identical with the distribution of mineralized outcrops containing copper minerals. Particularly, the highest anomalous part including anomalies of over 2,500 ppm Cu covers MA-2, MA-3 and MA-4 mineralized outcrops which are accompanied by abundant secondary copper minerals. The intensity of anomaly is obviously in proportion to the Cu content of the outcrops.

The evident correlation between the mineralized and geochemical anomalous zones in the Manikbel area is considered to be caused by the high sampling density although high Cu content is also one of the reason. The high sampling density seems to have separated the mineralized zone from non-mineralized area. For dissemination and/or network type of ore deposits, therefore, it is considered to be possible that the geochemical soil survey with the high sampling density can define the extent of mineralized zone with a higher accuracy.

In the Layacan area, two anomalous zones were recognized but compared with the Manikbel area both zones are of weak anomalies. The correlation between the mineralized zone and the anomalous zones is not as clear as that of the Manikbel area. This may be due to poor Cu mineralization and the mineralized zones distributed in this area are veins of extremely narrow lateral extension. In the Layacan area, the most efficient method of the geochemical prospecting is the systematic grid-sampling with a short interval between each sampling site.

PART Ⅲ GEOPHYSICAL SURVEY

1. GENERAL REMARKS

From the second phase of the geological and geochemical detailed survey in the Bucloc, Lacub, Malibcong and Ableg areas, Cu-Zn geochemical anomalies and network-dissemination type mineralization zones were comfirmed in the Manikbel area.

Prior to this project, the geological and geochemical survey, and 6 hole's drillings, had been conducted in a part of this mineralized zone by the Bureau of Mines and Geo-Science. However the whole aspect of mineralization had not been clarified.

In the third phase the induced polarization and complex resistivity survey were carried out to delineate mineralized zones, mainly to show sulfide minerals. A complex resistivity survey was performed with assistance from ZERO (Zonge Engineering and Research Organization), U.S.A.

2. OUTLINE OF SURVEY

2–1 Survey Instruments

2–1–1 Instruments for IP Method

IP transmitter — Model CH-T7802 and CH-505 by Chiba Electronics Co., Japan
Maximum output power 2.5A, 800V

Engine generator — Model 421 by Geotronics Inc., U.S.A.
Maximum output power 2 kw, 400 Hz, 115V

IP receiver — Model YDC-7505-B by Yokohama Electronic Co., Japan
Model CH-R7801 by Chiba Electronics Co., Japan

IP checker — Model YN-502 by Yokohama Electronics Co., Japan

2–1–2 Instruments for Physical Property Measurement

Transmitter — Model 801 by Burr-Brown Research Co., U.S.A.
Output frequency 0.01 Hz – 1,100 Hz
Output current 1μA – 11mA

Receiver — Model YDC-434 by Yokohama Electronic Co., Japan
Receiving frequency 0.1 Hz, 0.3 Hz, 1 Hz, 3 Hz
Input impedance 10M-ohm

2–1–3 Instruments for Complex Resistivity Method

CR receiver — Model GDP-12/2G by Zonge Engineering, U.S.A.
" CAP-12 "
" ISO-2 "
" FP-1 "
" EL-12 "
" VDB-2/3 "
Model 212 by Tectronix, U.S.A.

CR transmitter — Model FT-4 Geotronics Inc., U.S.A.
maximum output 4A, 800V
Model B-2 Geotronics Inc., U.S.A.
maximum output 3 Kw, 400 Hz, 115 V

2–2 Measurement

Eight survey lines were established after a discussion with the geological survey team on the basis of geochemical data, geology and topographic conditions. Seven of the lines were spaced 250 m apart oriented in the direction of N74 E with the other line oriented in the normal direction to them. For the survey a Ushikata pocket compass and 100 m measuring tape were used. The open traverses were run with the survey points set at a horizontal distance of 100 m. On Line C, D and E for the SIP method, additional three lines were cut on the north side at a distance of 30 m and parallel to each.

Survey points in the east-west lines were numbered starting from the west end station 0 (survey point), which is designated as the first point. For the north-south line, the same procedure was done with station 0 located at the north end.

A cardinal point was set at a distance of 90 m to the upper stream from the intersection of Manikbel River and its branch, with the point set at station 12.5 of Line H and station 15 of Line F. A elevation of the cardinal point was taken from 1:50,000 scale map, which gave the altitude of 470 m.

2–3 Outline of Geology

The geology of the survey area is characterized by andesitic rocks of the Licuan Group Formation II classified as Late Eocene and batholith-shaped plutonic rocks of Miocene intruding into andesitic rocks. The geophysical exploration area is underlain by andesite lava and quartz diorite intruding into this lava, and both of them are intruded by dykes of quartz diorite porphyry and dacite everywhere.

Quartz diorite is mainly exposed widely in the northeastern part of the survey area, the middle stream of Mamising River and the upper portion of Manikbel River. Generally this rock is of medium-grained and holocrystalline with dissemination of a large quantity of fine grained pyrite. Many fine fissures, which are often filled with fine-grained pyrite and quartz veinlets and/or occasionally clay occurred in marginal part of quartz diorite.

Andesite lavas are distributed from the central part to the southwestern part of the area, and at relatively higher portion of topography in the northeastern part. They are more or less subjected to a silicification and alter to hornfels by the effect of a intrustion of quartz diorite. A large quantity of fissures filled with a fine-grained pyrite and quartz, are recongnized in the lava.

Dykes of quartz diorite porphyry and dacite, trending WNW-ESE intrude into quartz

diorite and andesite lava in many places. They are occasionally accompanied by a small amount of pyrite dissemination, and generally their alteration are weaker than quartz diorite.

Copper mineralization observed in this survey area is of porphyry copper disseminated type containing a slight amount of chalcopyrite and pyrite. The mineralization is found mainly in quartz diorite distributed in the northwestern part of the area, and especially developes along the boundary between quartz diorite and andesite lava.

Table III–1 List of survey line

LINE	LENGTH	INTERVAL	SPACE FACTOR
A	2.5	100 m	n = 1 ~ 5
B	4.0	"	"
C	4.0 (1.6)	"	"
D	4.0 (1.6)	"	"
E	4.0 (1.6)	"	"
F	4.0	"	"
G	2.5	"	"
H	1.5	"	"
Total	26.5 (4.8) Km		

* ( ) : For Complex Resistivity Survey

3. METHOD OF SURVEY

The variable frequency IP method with a dipole-dipole array, which has been generally used for prospecting porphyry copper deposits and CR (complex resistivity) method, were used in this survey.

3–1 IP Method

IP method is conducted by supplying AC current I_{AC} into the ground through a pair of current electrodes (C_1, C_2) with another potential electrodes (P_1, P_2) detecting the potential difference V_{AC}.

In this case, the apparent resistivity ρ_{AC} of the ground is calculated by the following equation.

$$\rho_{AC} = K \cdot V_{AC} / I_{AC}$$

K is a geometrical factor, and when a electrode distance and a electrode space factor is "a" and "n" respectively, K is as follows.

$$K = 2\pi / \left(\frac{1}{C_1 P_1} - \frac{1}{C_1 P_2} - \frac{1}{C_2 P_1} + \frac{1}{C_2 P_2} \right)$$

$$= \pi n (n+1) (n+2) a$$

In this survey, "a" is 100 m and "n" is 1 to 5. The method used in plotting the data is shown in Fig. III–1.

After reading the potential difference V, keeping the current at constant, and by lowering the frequency close to DC current, the deviation of the apparent resistivity due to frequency change is directly taken. This deviation is called as the frequency effect (FE) and it is defined by the equation:

$$FE = \frac{V_{DC} - V_{AC}}{V_{AC}} \times 100\,(\%) = \frac{\rho_{DC} - \rho_{AC}}{\rho_{AC}} \times 100\,(\%)$$

In this survey, the frequencies used are 3.0 and 0.3Hz.

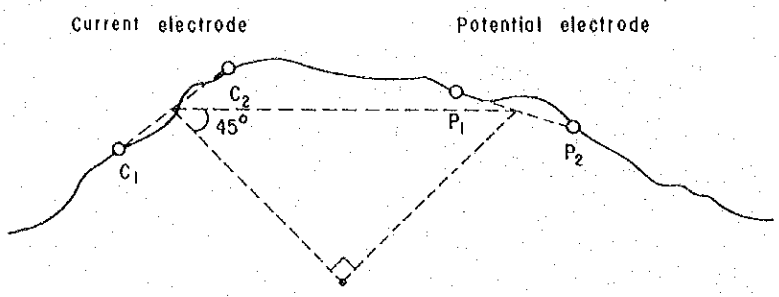

Fig. III–1 Plotting Method

Terrain Correction

As FE is a deviation of apparent resistivity, it is less affected by topography. But as a geometrical factor K is assumed on the basis of half-infinite plane, the apparent resistivity is affected by the topography depending on the locations of electrodes. That is, resistivity will be detected high beneath a hill and low beneath a valley.

For the purpose of rejecting the topographic effect quantitatively, a method using conductive paper was adopted. This method is done by using a conductive sheet of constant resistivity and cutting the paper simulating a scaled topography. A weak current is passed through the simulated topographic section and potentials are measured.

As this correction is performed on the basis of the two-dimensional half-infinite plain topography, it is impossible to eliminate the effect in case that IP survey lines are parallel to a ridge or a creek. The effect of small topographic changes or the changes of the resistivity near the surface can not also be corrected.

In the case of the area where the mountain is perpendicular to the survey line, there is a tendency that the effect of the topography can possibly be eliminated.

As the topography in the survey area is very steep and so rugged, the apparent resistivity is affected by the changes of the topography. Then, two-dimensional terrain correction had to be applied to all IP survey lines.

3–2 Complex Resistivity Method

Complex resistivity method is a useful exploration tool detecting a complex resistivity spectra of the earth using multiple frequencies. The method has three advantages; noise rejection, electromagnetic coupling removal, and complete spectral identification. These advantages increase the effect of skin depth and would enable the possibility to distinguish the type of mineral that induced the polarization.

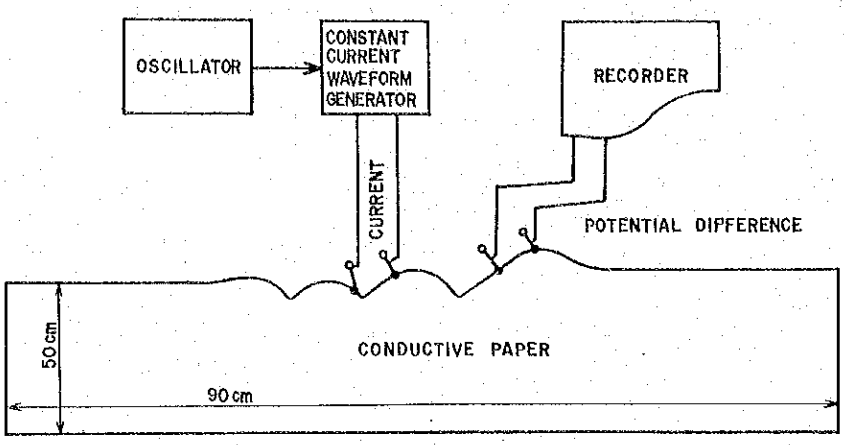

Fig. III–2 Block Diagram of Terrain Correction

The observation is done by supplying a square-wave current into the ground through a pair of electrodes and amplifying a potential difference by a pre-amplifier, which is then fed to channel 1 of a receiver through an isoamplifier. Simultaneously, current from a transmitter is introduced through the other channel via a standard 0.1Ω resistance. These signals pass through a, b and c analog circuit, and the results are displayed on a front panel after digital processing and frequency analysis in circuit d and e. After all of these procedures are finished in one frequency, the same procedures are repeated in another frequency. The circuits of a GDP-12 receiver are as follows.

a. Differential amplifier for channels 1 and 2.
b. SP rejection circuit of channel 1
c. Low pass filter, 50/60 Hz notch filter
d. Digitizing circuit —— 12 bit A/D convert sampling, and stacking
e. FFT circuit
f. Deconvolution circuit
g. Calculation circuit of complex resistivity and phase

Data processing is done using the cassette tape obtained from the field observation. A Cole-Cole figure is made, and apparent resistivity and phase are calculated out by data processing. These values are displayed on a psuedo-section map the same as IP plotting.

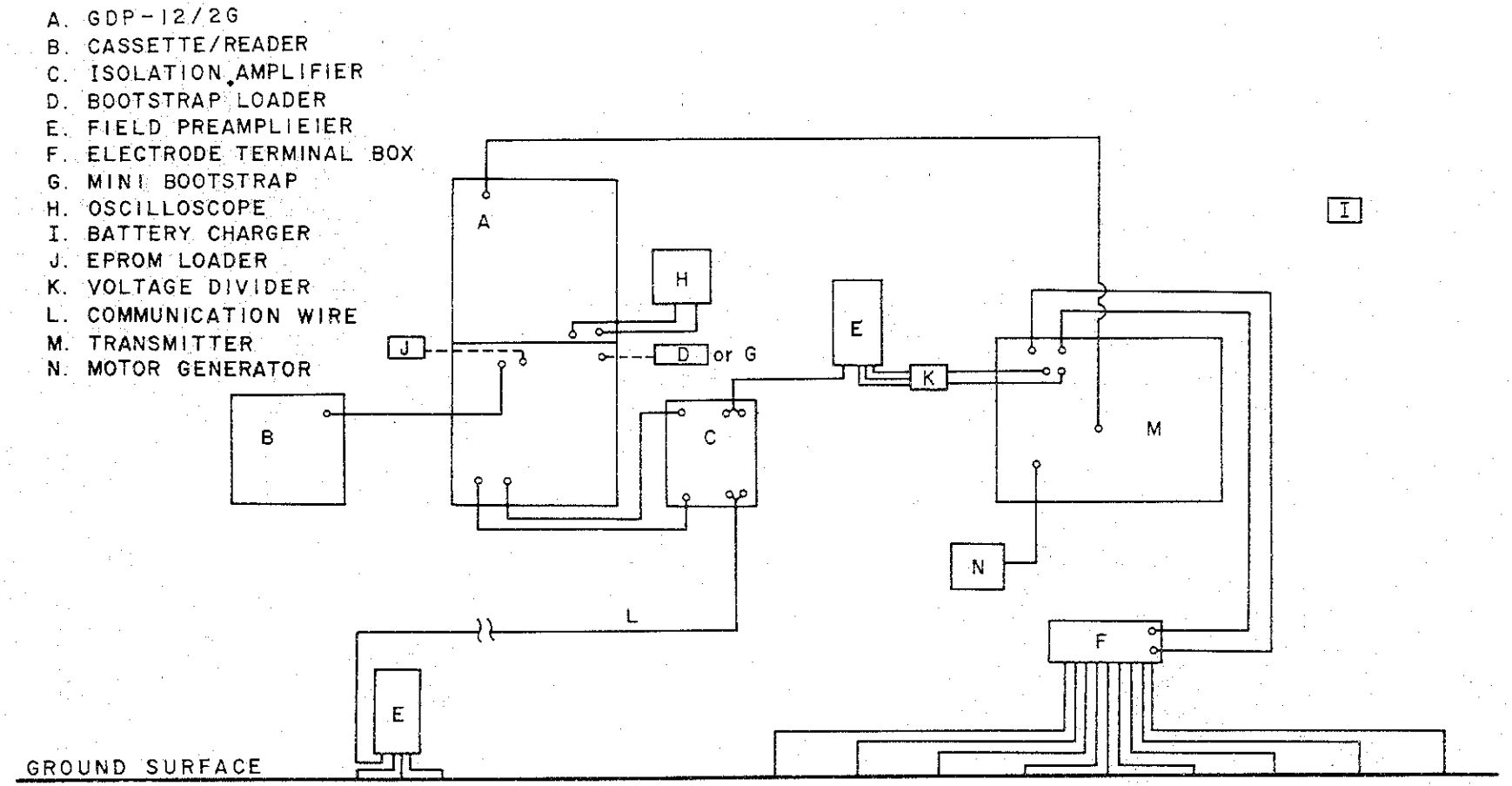

Fig. III–3 Block Diagram of CR System

4. ANALYSIS OF SURVEY RESULTS

4–1 Analysis of IP Results

4–1–1 Analysis of IP Profiles

From the FE values obtained from the survey area, 3 anomaly zones were interpreted. The range of FE values shown below were chosen to describe these anomalies, which are referred to as the Western, Central and Eastern anomaly zones respectively.

FE (Frequency Effect)

Low FE anomaly	Middle FE anomaly	High FE anomaly
(Type C)	(Type B)	(Type A)
3.0% – 5%	5.1% – 7.0%	7.0% <

AR (Apparent Resistivity)

Low AR	Middle AR	High AR
less than 500Ωm	501Ωm – 1000Ωm	1000Ωm<

Line A

In the Western anomaly zone, an anomaly on the west of station 2 indicates the existence of a FE response body of Type B. An anomaly between station 2 and station 12 is separated by background FE response bodies that are presumably located near the surface between station 3 and station 4, and between station 6 and station 8. This region is mainly underlain by FE response of Type B.

In the Central anomaly zone, a high FE anomaly is widely found between stations 13 and 17 at n=1, to between stations 15 and 23 at n=5. This anomaly shows that a Type A mass centered at stations 16 and 17 extends to the east side of line. Another horizontal tabular response body of Type B is expected at shallow depths beneath stations 19 through 25. An apparent resistivity is low and middle excepting high AR at depths between stations 5 and 14. The region of high AR nearly corresponds to the FE anomaly zone of Type C and B, while low-middle AR zone correspond to the anomaly zone of Type A.

Line B

In the Western anomaly, FE anomaly which shows the "pantleg" between stations 9 and 11 suggests that the tabular FE response body exists around station 10. The Western anomaly zone's area as a whole consists of the FE response mass of Type C excepting

the shallow part between stations 4 and 5, and between stations 11 and 12. In the Central anomaly zone, the tabular FE response body of Type A is expected at shallow depth between stations 18 and 19, and the vertical FE response body of Type A is expected at depths beneath stations 20 through 23, judging from the FE contour.

An anomaly on the east of station 33 does not give the whole aspect of the Eastern anomaly zone, because it is located at the end of the survey line. Nevertheless, it suggests FE response body of Type A existing up to depths from the surface. High AR is recognized at depths west of station 13, and between stations 23 and 33.

The distribution area of low-middle AR harmonically corresponds to the FE anomaly zone.

Line C

The scale of the Western anomaly is smaller than that of Line A and Line B, but a high FE anomaly between stations 3 and 6 indicates that tabular FE response bodies of Type A are expected near the surface of station 4, and beneath stations 6 and 7.

FE value of the Central anomaly zone decreases a little in comparison with that of Line A and Line B. The "pantleg" shape of middle FE anomaly between stations 19 and 20 may result from the reduction by background FE body which exists on the surface around station 19.

The pattern of the Eastern anomaly is nearly similar with that of Line B and the broad FE response body is expected to extend at shallow depth from station 34 to 38.

The pattern of AR has a same tendency to that of Line B. The low AR associated with high FE is detected in the west and central of survey line. The high AR is uniformly distributed at depths excepting from station 31 to 34.

Line D

The FE contour of the Western anomaly is nearly as similar as that of Line C. This anomaly may be due to the tabular FE response of Type A dipping westwards which presumably exists on the west of station 3. The distribution area of the Central anomaly shifts to the west side in comparison with that of Line C. The FE response of Type B is expected near the surface around station 24 to 25.

The Eastern anomaly, the distribution area of which is narrow compared with that of Line A, B and C, indicates the FE response of Type A dipping eastwards from the surface

to depth between stations 34 and 36. This area consists of low-middle AR in the upper portion and high AR is dominated in the lower portion.

Line E

The Western anomaly zone, which shows low-middle FE, shifts about 300 m to 400 m to the west side as compared with those of Line C and Line D. The center of anomaly zone is expected on the west of station 2.

In the Central anomaly zone, two typical "pantleg" anomalies are recognized between stations 11 and 12, and station 17 to 19, respectively. The former indicate the existence of FE response body dipping eastwards, and the latter may be expected due to the FE response which horizontally lie near the surface between stations 17 and 19.

The Eastern anomaly has a tendency to become smaller and narrower at depths. The FE response body of flat structure is assumed near the surface from station 34 to 35 and other FE small response body is expected to exist dipping to the west side.

The high AR is dominant to the east of station 13 and distributed at depths except that other high AR is detected near the surface to the west of station 13.

Line F

Only the Central anomaly zone is recognized and the Western and the Eastern anomaly zone, which are widely distributed in Lines A, B, C, D and E, are not detected. The anomaly extending from n=1 of stations 1 through 3 (Stations 1 – 3) to n=5 of stations 4 and 5 indicates the existence of the small FE response body in and around station 2.

The Central anomaly zone, which is detected from n=1 of stations 17 – 20 to n=5 of stations 15 – 21, become small as compared with those of Lines A, B, C, D and E. This anomaly indicates that FE response body dipping westwards lies between stations 17 and 19.

Other two anomaly are partly found between stations 32 and 33, and around station 38. These anomaly may be expected to be occurred by the vein-type FE responses which exist around station 32 and station 38, respectively.

The pattern of AR is the same as that of Line F, but between stations 7 and 15, the low-middle AR less than 1,000 Ωm is distributed more widely than that on Line F.

Line G

This line is 500 m shorter on the west side and 1,000 m on the east side than Lines B,

C, D, E and F. The low FE anomaly to the west of station 4, middle FE anomaly between stations 9 and 15, and another low FE anomaly to the east of station 18 are recognized.

The first may indicate that the tabular FE response dipping eastward exists near the surface from station 1 to 2. The second, which shows "pantleg", may due to the FE response dipping eastwards, located near the surface of station 11 to station 12. The third is obscure in its anomaly type, because it is located in the end of line. The high AR is dominantly distributed in the lower part on this line.

Line H

This line is perpendicular to Lines A, ... etc., and pass station 15 of each line.

Three high anomaly zones are detected; to the north of station 5, between stations 6 and 8, and between stations 9 and 11. The anomaly to the north of station 5 may correspond to that of Lines A, B and C. The anomaly between stations 6 and 8 may be expected due to the tabular FE response body dipping northwards which is located on the surface around station 8, and is consistent with the high FE zone on Line D.

The anomaly detected between stations 8 and 11 may be induced by the FE response body dipping northwards, originated from station 11.

4–1–2 Plane Analysis

From each IP profile, the values at n=1, 3 and 5 were derived, then three types of map were completed. Due to rugged topography, these maps do not indicate the same level plane, but show the plane from 100 m to 300 m below the surface.

The objective of this analysis is to delineate the horizontal spread of the mineralized zone and if possible to evaluate its dip and direction.

FE

Three anomaly zones of more than 5 percent FE mentioned in the analysis of IP profile (the Western, the Central, the Eastern anomaly zone), are found on each plane of n=1, 3 and 5. The Western anomaly zone, (the center of which is located in the vicinities of stations 3 to 5 on Line C and stations 3 to 4 on Line D), roughly distributes to a N-S to NW-SE trend at n=1. In the plane of n=3, this anomaly extends to the E-W direction and is divided into two small anomalies, west and east side. Its intensity decreases going deeper, and this indicates that the FE response body may be present at shallower depth than n=3.

The Central anomaly zone, the biggest one, is distributed from the surface to depths

Apparent Resistivity (Ω–m)

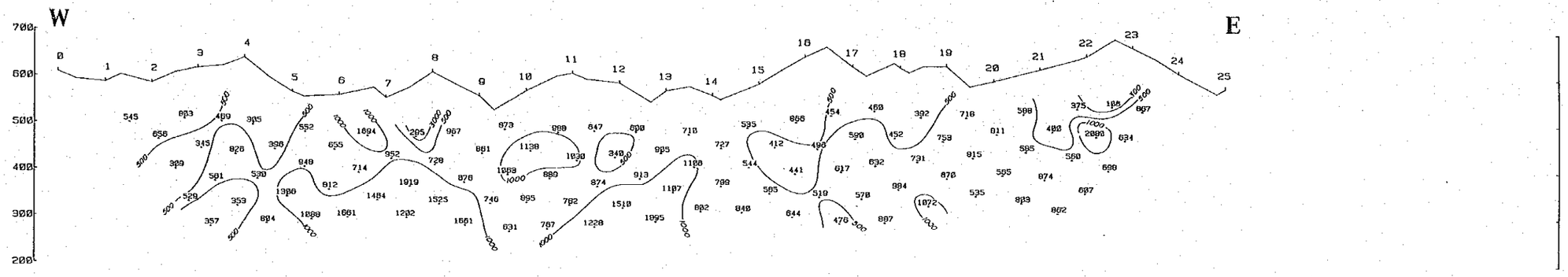

Frequency Effect (%)

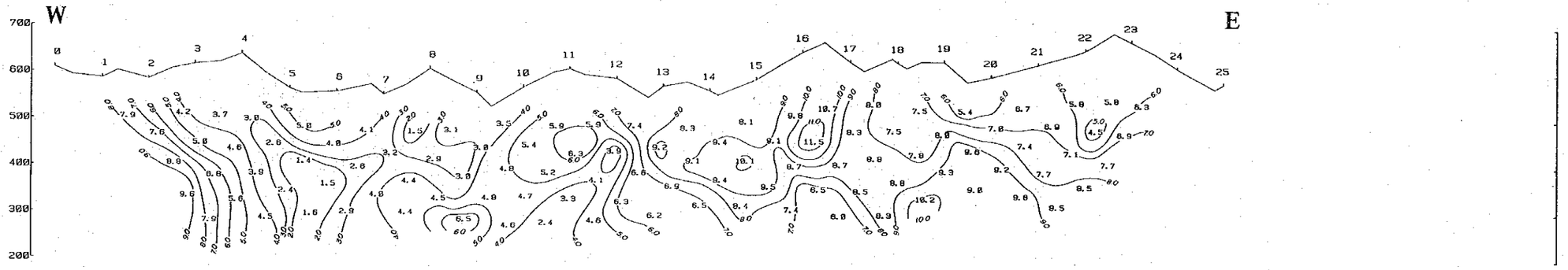

LINE A

Fig. III–4–1 IP Profile

Apparent Resistivity (Ω–m)

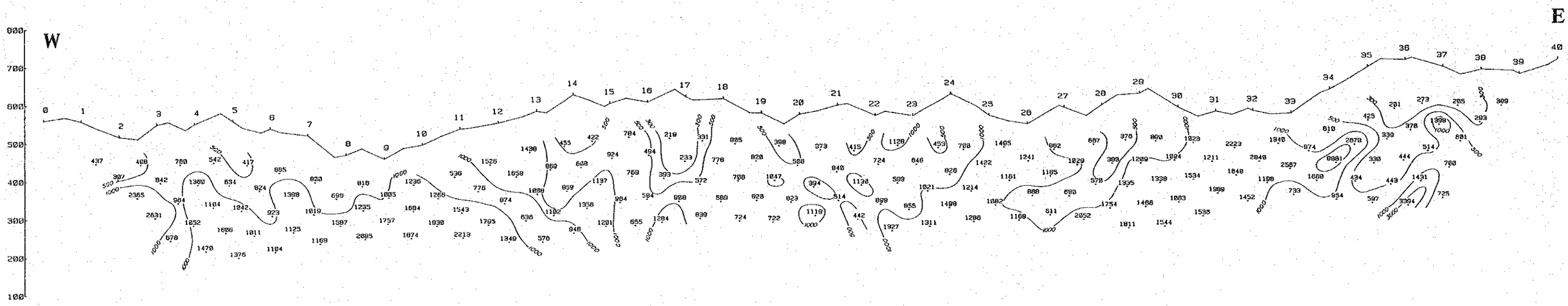

Frequency Effect (%)

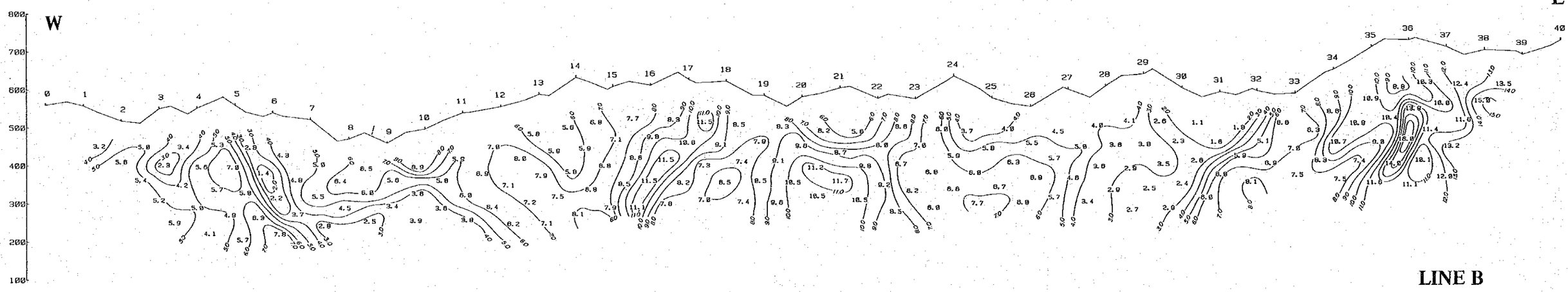

LINE B

Fig. III–4–2 IP Profile

Apparent Resistivity (Ω–m)

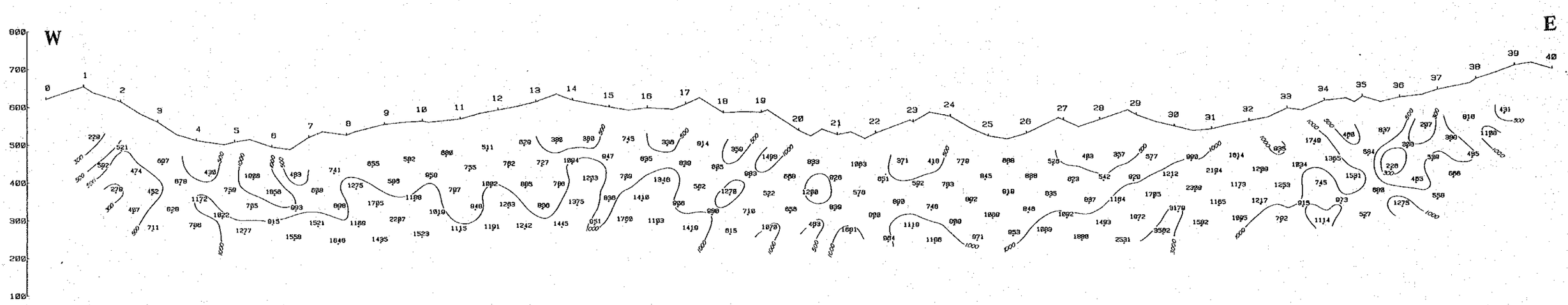

Frequency Effect (%)

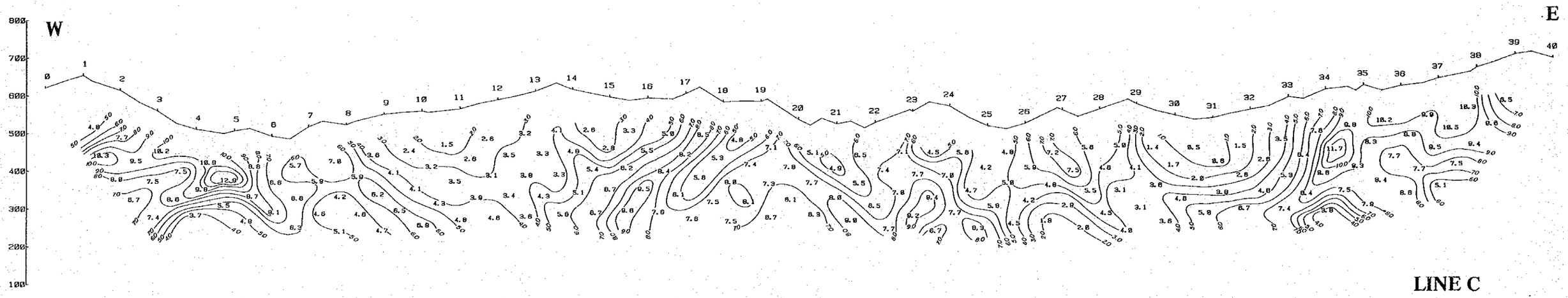

LINE C

Fig. III–4–3 IP Profile

Apparent Resistivity (Ω–m)

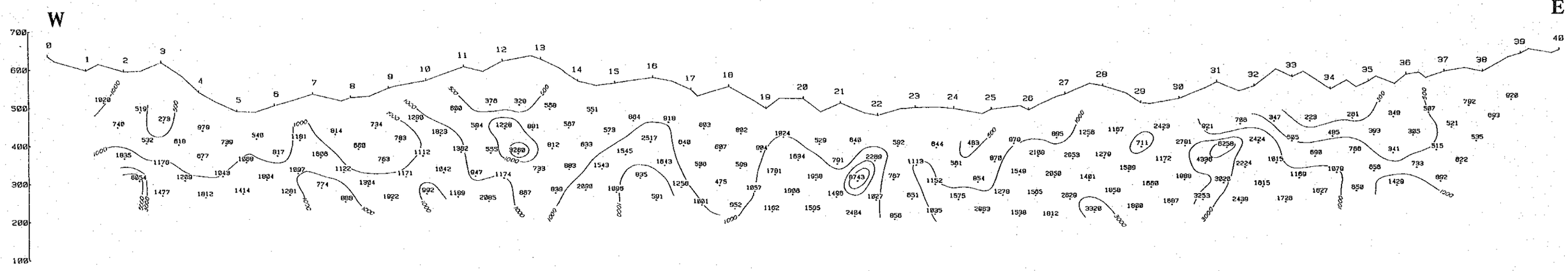

Frequency Effect (%)

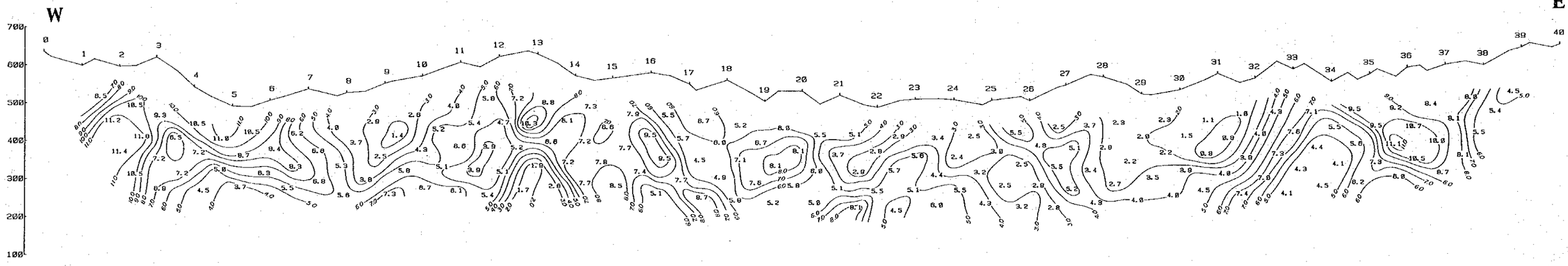

LINE D

Fig. III–4–4 IP Profile

Apparent Resistivity (Ω–m)

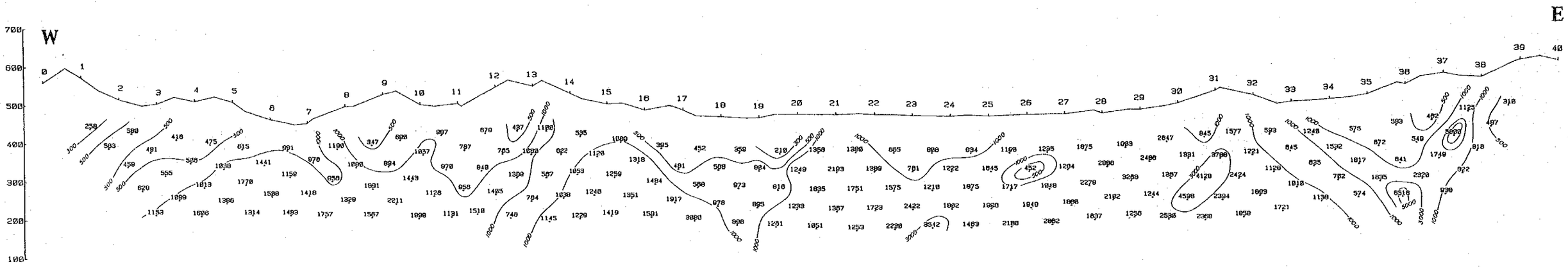

Frequency Effect (%)

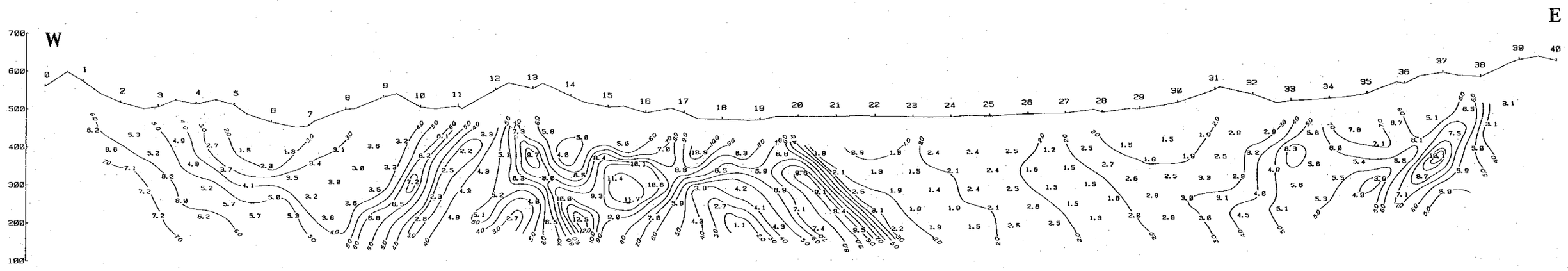

LINE E

Fig. III–4–5 IP Profile

Apparent Resistivity (Ω–m)

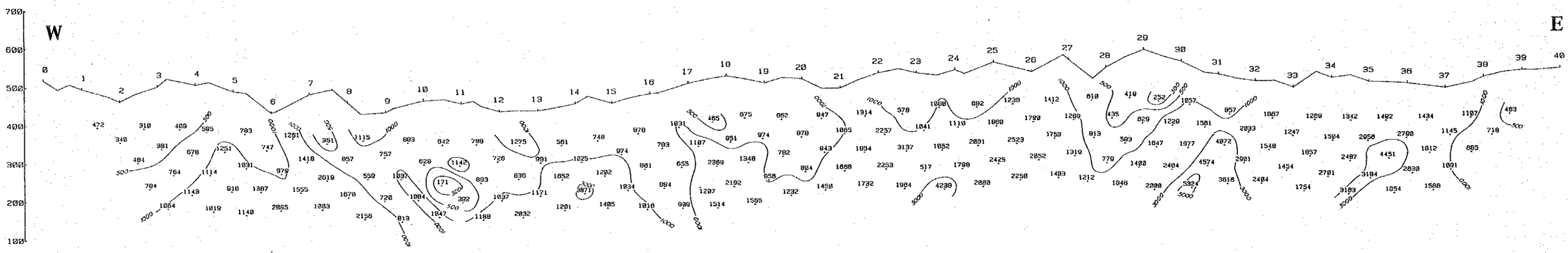

Frequency Effect (%)

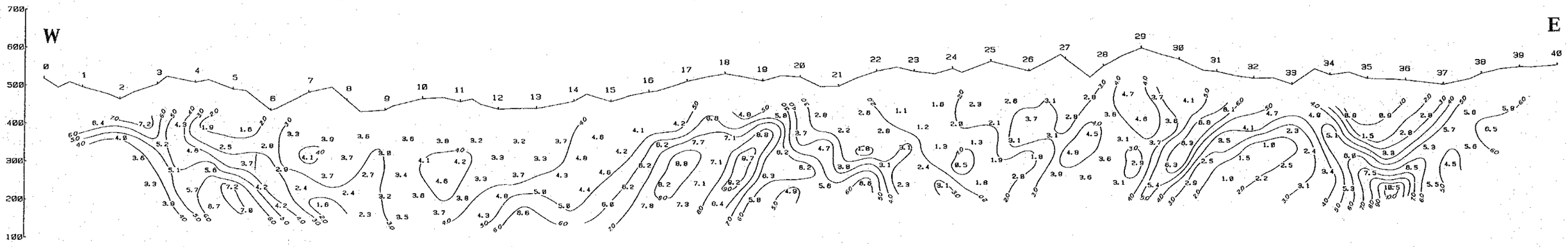

LINE F

Fig. III–4–6 IP Profile

Apparent Resistivity (Ω–m)

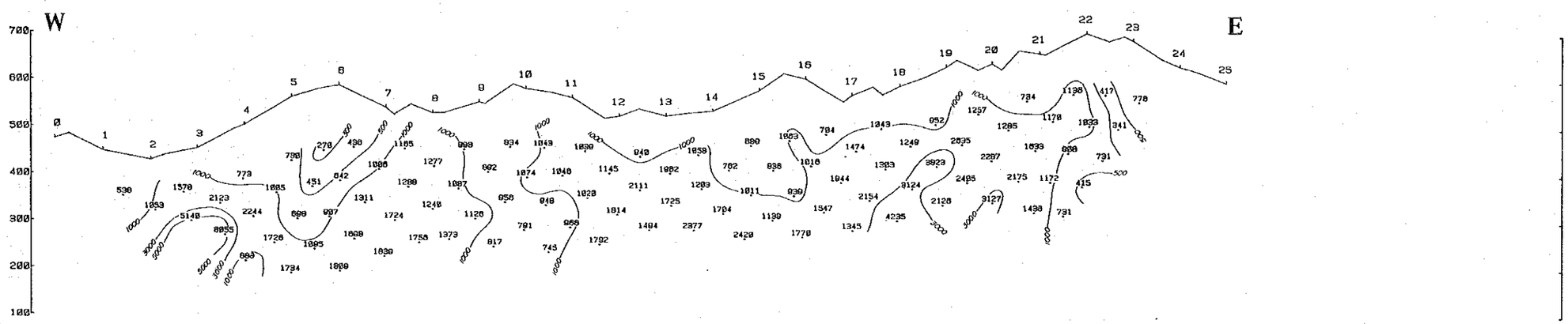

Frequency Effect (%)

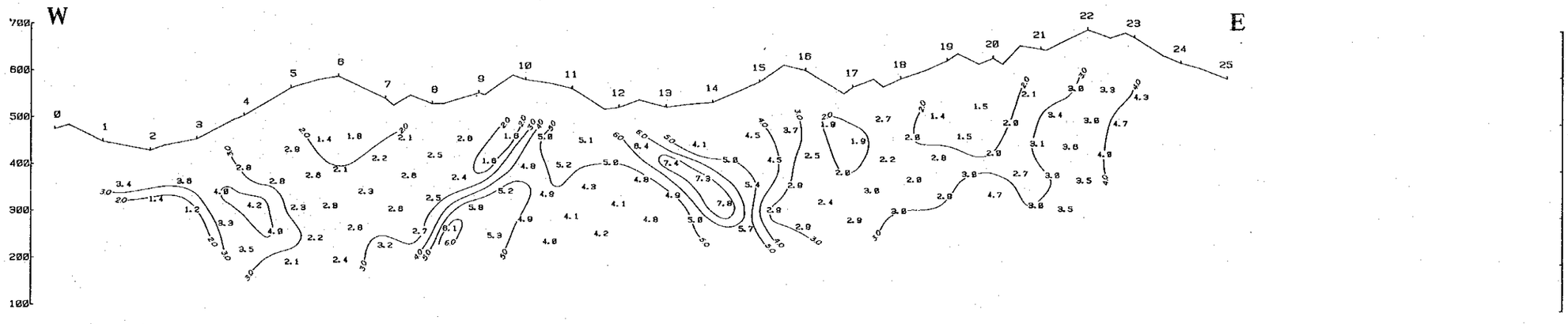

LINE G

Fig. III–4–7 IP Profile

Apparent Resistivity (Ω–m)

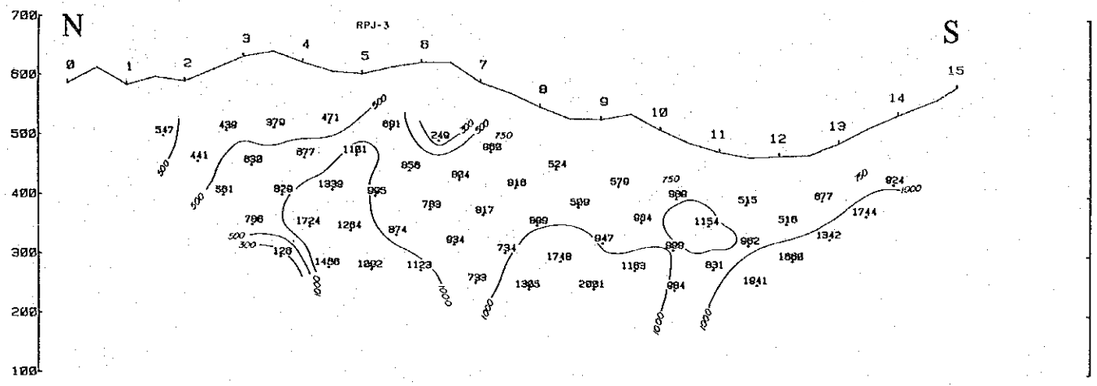

Frequency Effect (%)

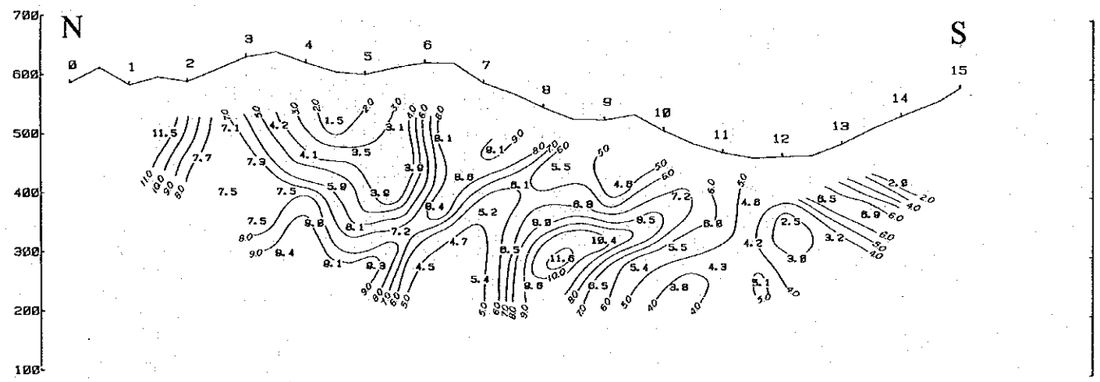

LINE H

Fig. III–4–8 IP Profile

in a mainly N-S trend. The anomaly zone of over 7 percent FE becomes wide to the north of Line D at n=3 and n=5, and is a little narrow at n=1. The high FE response body is anticipated to exist at deeper zone than n=3. Also the anomaly's intensity becomes stronger northward and weak southward.

The Eastern anomaly zone is found in a NW-SE, trending to the north of Line F. This anomaly extends north in the same direction as the Central anomaly zone, although its intensity gradually decrease with depth in the south.

Apparent Resistivity

A low-middle resistivity zone of less than 1,000 ohm-m is widely distributed at n=1, although a high resistivity zone of more than 1,000 ohm-m is sporadically distributed trending N-S.

In the plane of n=3, a high resistivity zone is widely distributed in a fan-shaped area streching to the south of station 23 through 33 on Line B, and an other high resistivity zone is found west of station 10 of each line. The low-middle resistivity zone is roughly coincident with the Central and Eastern FE anomaly zones.

In the plane of n=5, a low-middle resistivity zone is found in three regions on Lines A, B and C; to the north of station 5, at the central part and on the east edge of each line. While high resistivity is dominant in other places.

The summary of plane analysis is as follows.

(1) Resistivity tends to become higher at depths and to the south in the survey area, and generally the FE anomaly zone is not coincident with the high resistivity zone.

(2) The low-middle resistivity zone is dominantly distributed at shallow depth, but continues deeper, and becoming wider to the north, in the central and eastern part of the survey area. From the plane analysis, the correlation of FE and resistivity value with the surface geology is shown below. From a comparison between geological column obtained from drillings (RPJ-1, RPJ-2, RPJ-3) and FE value, andesite detected by drillings (RPJ-1, RPJ-2) is correlative with high resistivity / high FE.

FE / Resistivity	Background FE (less than 3%)	Low-middle FE (3 – 7%)	High FE (more than 7%)
Low-middle resistivity (less than 1,000 Ωm)	quartz diorite (B) andesite (A)	quartz diorite (C) andesite (B)	quartz diorite (D) andesite (C)
High resistivity (more than 1,000Ωm)	quartz diorite (A)		(andesite (D))

The distribution areas of these classified rocks are as follows.

◦Quartz diorite (A)

This rock is widely distributed in the area between the Eastern and the Central anomaly zone, being dominant south of Line D. There is almost no change in FE and resistivity value from the surface to depth (n=5). It is assumed that this rock may be hard and compact, and contains little sulfides to great depths.

◦Quartz diorite (B)

This rock is distributed near the surface in the area between the Western and the Central anomaly zone, and between the Central and the Eastern anomaly zone on Lines B and C. Quartz diorite (A) underlies this rock. This rock is inferred to be the weathered layer of quartz diorite (A) and to have little sulfides.

◦Quartz diorite (C)

This rock is mainly seen in the surrounding of the Western, the Central and the Eastern anomaly zone, and shift generally into high resistivity rock in the deeper portion of the ground. Quartz diorite (C) is not as hard and compact a rock as other similar rock types in the study area, associated with a slight fissure, along which some sulfide mineralization has occurred.

◦Quartz diorite (D)

This rock is found within the Western and Eastern anomaly zone north of the survey area, and low resistivity continues deeper in the Eastern anomaly zone, although in the Western anomaly zone, the resistivity becomes higher at depth. This high FE value makes it appear that it contains a large amount of pyrite, and the low resistivity at the depths of the Eastern anomaly zone suggests that there are many fissures and fractures in this rock.

However, granodiorite within the Western anomaly zone is inferred to be hard and compact at depths.

◦ Andesite (A)

This rock is found only on the west side of Lines F and G, with no mineralization.

◦ Andesite (B)

This rock is distributed partly in the eastern edge of Line A and central part of Line D. It has slight fissures and fractures such as quartz diorite (C), and the weak pyrite mineralization that may occur along them.

◦ Andesite (C)

This rock is well-distributed correlating very closely with the Central anomaly zone, especially in the middle part of the zone along Lines A, B and C. The anomaly contour correlates very well with the andisite (C) distribution defined by the geology and drilling. Low resistivity to depths indicates that many fissures and cracks developed to the deeper zone, and the high FE value shows that this rock contains a relatively large amount of pyrite.

◦ Andesite (D)

This rock was detected by drilling holes RPJ-2 and RPJ-3, with pyrite veinlets which roughly correlate with the high resistivity and FE. A great deal of film-shaped pyrite occurred in this rock, which seems to induce the high FE.

4–1–3 Physical Property Measurement

Outline

Physical properties measured at the surface do not necessarily indicate the real properties of rocks, ore deposits, etc., because these are affected by overburden, weathered layer and underground water. Therefore, it is important to know the underground physical properties as close as possible for geophysical exploration. There are two ways to accomplish this purpose, one is an in-situ survey, and the other is the measurement of the physical property of rock samples in the laboratory.

In this survey, the latter method was applied because of inadequate outcrops in the survey area. Forty two comparatively fresh rock samples were collected for the resistivity and FE measurements.

The Method of Measurement

In the laboratory, prior to the physical property measurements, the rock samples were cut into rectangular blocks. It is desirable to have the specimens in the same condition as at the time of sampling, so the dried samples were placed in a depressurized water tank to

subject all of them to similar conditions before the measurements. The frequency used was 0.3 and 3 Hz.

The resistivity is calculated from the following equation:

$$\rho = \frac{a_1 \times a_2}{\ell} \times \frac{V}{I}$$

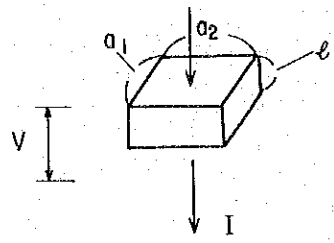

Where, ℓ is the length of the sample, a, and a_2 are the depth of the sample, V is the potential difference and I is current.

Results of Measurements

The results are shown in Table III–2. The resistivities of specimens range from 639 ohm-m to 50600 ohm-m and FE are 1.4 % to 11.5 %.

(Resistivity)

The sample types are andesite, granodiorite, and quartz diorite porphyry, and the average resistivities are as follows.

Andesite ..... 4,030 ohm-m

Granodiorite ..... 8,400 ohm-m

Quartz diorite porphyry. 6,300 ohm-m

The resistivities of the samples are higher than which were observed in the field. The possible reasons for these differences are :

1. Apparent resistivity of the rock in the field is effected by low resistivity porous materials like overburden and weathered layers.
2. specimens only represent a small part of the rock mass, and generally correspond to a hard compact part of the rock.
3. Andesite and granodiorite rock mass in-situ, contain fractures which are filled with extremely low resistivity materials such as clay, sulfide, and underground water.

(FE)

In general it was found that there is a correlation of the FE value with the volume content of sulfide. In this survey, the analysis of sulfur for ten selected specimens from the total collected samples, was done and the correlation of FE value with sulfide was investigated. These results are shown in Table III–3. This correlation is not clear, and the negative results

Table III–2 FE and Resistivity of Rock Samples

Location and Sample No.	FE (%)	ρ (Ωm)	Rock Name
A–5	3.2	4,500	quartz diorite porphyry dyke
A–9.5	4.8	6,320	quartz diorite porphyry dyke
B–8	1.9	3,170	quartz diorite porphyry dyke
B–19.5	3.0	3,640	andesite
B–27.5	5.1	12,800	granodiorite
B–30.5	5.0	2,820	granodiorite
B–32	3.1	18,800	granodiorite
C–4	8.0	8,170	quartz diorite porphyry dyke
C–6.5	2.9	11,900	granodiorite
C–11	2.4	2,300	quartz diorite porphyry dyke
C–15.5	8.5	29,800	andesite
C–16.5	4.5	38,600	andesite
C–18	1.8	4,350	andesite
C–20	2.4	4,190	andesite
C–20.25	9.6	9,490	andesite
C–26	2.5	2,240	andesite
C–36	2.0	4,770	andesite
D–0.5	3.5	2,530	quartz diorite porphyry dyke
D–7.5	2.0	5,130	quartz diorite porphyry dyke
D–8.5	3.6	2,730	andesite
D–11.5A	2.7	2,430	andesite
D–11.5	2.8	2,150	andesite
D–13.75	2.8	16,500	andesite
D–14.5	1.4	29,700	andesite
D–17	3.0	1,520	andesite
D–17.20	3.0	3,780	andesite
D–19A	5.0	639	andesite
D–19	3.3	7,180	andesite
D–20.5	6.0	19,600	andesite
D–31.2	2.5	36,700	quartz diorite porphyry dyke
D–35.2	1.8	2,230	quartz diorite porphyry dyke
D–35.5	2.4	5,060	quartz diorite porphyry dyke
E–8.5A	4.3	4,610	andesite
E–8.5	11.5	15,700	quartz diorite porphyry dyke
E–11	2.4	1.480	andesite
E–11.20	4.0	5,730	andesite
E–14.5	3.7	21,500	andesite
E–32.3	2.9	3,680	quartz diorite porphyry dyke
E–40	2.1	50,600	quartz diorite porphyry dyke
F–2	1.8	15,400	andesite
F–28	9.6	5,790	granodiorite
G–21	5.5	7,740	granodiorite

are assumed to be caused by the different type of mineralization. From detailed observations, two types of mineralization of the analyzed specimens were determined.

There are :

Type 1. The film-shaped sulfides distributed along the fissures of the specimen.

Type 2. The sulfide disseminated in the specimen.

Table III–3 Result of Chemical Analysis for Rock Samples

Sample No.	FE (%)	Cu (ppm)	S (%)	Rock Name
A–9.5	4.8	128	0.21	quartz diorite porphyry dyke
B–8	1.9	76	0.16	"
C–6.5	2.9	92	0.18	grannodiorite
C–15.5	8.5	124	0.09	andesite
C–16.5	4.5	94	0.05	andesite
D–8.5	3.6	103	0.24	andesite
D–13.75	2.8	47	0.05	andesite
D–17	3.0	42	0.29	andesite
E–11	2.4	100	0.51	andesite
E–14.5	3.7	59	0.06	andesite

The specimens of Type 1 are typically A-9.5 (4.8%), C-15.5 (8.5%) and C-16.5 (4.5%) and for Type 2 are B-8 (1.9%), C-6.5 (2.9%) and D-13.75 (2.8%). These results indicate that the film of sulfides (Type 1) induce a frequency effect, more than the sulfide dissemination of Type 2.

4–1–4 Results of Model Calculation

In analyzing the forms and strength of the geophysical anomalies, the results are often checked and compared with the results of the model calculation, and also with the geological structure in order to establish a hypothesis.

In the IP method, various model calculations were conducted from the dipole-dipole electrode array, but the data observed were affected by various anomalies so that general factors are considered to establish good results or assumptions.

From the B survey lines, 3 lines were selected for quantitative analysis, they are Line C, D and E, where high FE anomalies were detected, and complex resistivity survey and drilling operations were conducted.

The structural model for each IP profile was considered, and to evaluate the validity of the structural assumption, the FE resistivity values were assigned to the different geological units of the model to establish an assumption.

For the calculation, each sections were divided into 1,400 grids and the assumed FE and resistivity values were assigned in each grid. The IBM 370/195 was used in the calculation by finite element method. The computer output printed out the assumed model form, FE and resistivity. The comparison between the calculated and actual section, especially, FE was evaluated and various parameters changed in order to approach the observed value. By this procedure it was possible to simulate the tendency and pattern of the actual structures, but they are so complicated and the combination of the geophysical properties that can be assumed are so many that it would be very difficult to conduct an ideal simulation. It was then assumed that the approximate values of the FE and resistivity are close to the observed values. For the calculation it is possible to set an assumption on the nine types of codes, but only six to seven codes were used.

4–2 Analysis of Complex Resistivity Results

Results of the complex resistivity survey conducted by Zonge Engineering and Research Organization are described below.

4–2–1 Results of Complex Resistivity Measurements on Rock Samples

Complex Resistivity measurements on five rock samples obtained from the field were performed. Table III–3 summarizes the results.

Table III–4 CR measurements on rock samples

Sample No.	PFE (%)	Resistivity (Ωm)	Polarization (MR)	Spectral Type	Rock Name
H–2110/long	25.3	80	154	aaA	Py/cpy in quartz vein in andesite
H–2110/short	26.4	230	178	AAB	
E–2167	1.6	5330	10	CCb	Tuff breccia
B–2106	3.9	7064	23	cbb	Granodiorite
G–2113	1.0	616	7	CCC	Quartz diorite
B–2116	1.4	349	7	CCB	Quartz diorite porphyry dyke

The mineralized sample (H–2110) was measured in two directions. The short direction provided an "electrode" type "A" response indicating that the mineral grains were relatively well-interconnected, and the sample was acting like a single metallic electrode. Measuring in the long direction provided a milder type "a" response, somewhat typical of samples with abundant pyrite/chalcopyrite. The low frequency tail is due either to alteration products or the massive nature of mineralization in the rock sample.

The other four samples provided type "c" responses of varying magnitude, typical of barren rocks of this type. The large response of B–2106 is probably due to layered silicates.

4–2–2 Analysis of Profiles and Planes

Apparent resistivity, polarization, FE and spectral profiles on Line C, D and E are shown in Fig. III–5–1 to 6 respectively. Fig. III–6–1 to 3 summarize the polarization data at n=1, 3 and 5 and Fig. III–6–4 to 6 are plots of spectral response at n=1, 3 and 5 respectively.

Line C

Apparent resistivity values are irregular along this line reflecting the effect of variable near-surface resistivities, topography and lateral contact features. The contact between quartz diorite and andesite occurring between stations 13 and 14 is not well-delineated, although a low-resistivity diagonal appears to originate from this contact.

Polarization values gradually increase going from west to east with the most intensive values occurring at depth beneath station 16. Both the resistivity and polarization values display a layered effect dipping toward the west.

The spectral type response conforms somewhat to the polarization picture, although similar spectral responses cut across differing resistivity and polarization features. The high frequency spectral responses show a division between type "b" responses to the east and type "c" responses to the west of station 14, which is roughly coincident with the quartz diorite-andesite contact.

The 0.125 Hz block displays additional character in the spectral signatures, and should probably be used for any attempt at mineral discrimination on all three lines. Since the spectra generated on this survey do not conform to our normal "textbook" porphyry copper spectra that are found in the southwestern United States, it is difficult to attach mineral characteristics to individual spectra, without drillhole confirmation on some typical spectral signatures. However, it is relatively certain that the type "B" responses centered

beneath stations 16 and 17 at depths are probably due to large concentrations of pyrite. The "pantleg" of type "C" response centered beneath stations 11 and 12 is probably due to a near-surface feature in that vicinity. This type of spectral signature seldom has sulfides associated with it.

Type "b" responses are very similar and probably show the effect of sulfides of unknown composition, although pyrite must be included.

As noted in the appendix summarizing the CR measurements on five rock samples, the response of the barren host material is basically a type "c" or "C". The quartz diorite and granodiorite samples provided steep "C" spectra similar to the responses observed to the west of station 14.

At this time it is not possible to differentiate between different sulfide responses to the east of station 14. It will be very useful to have information on the drillhole results and some core samples for measurement to correlate with field results in this area.

Line D

Again on this line, the apparent resistivity values are irregular and do not outline any major structural features, and the polarization values generally increase toward the east.

This line was run over the andesite host, and spectral responses indicate this by providing type "b" or "B" responses over most of the line. Some type "c" spectra encroach on the western end and are probably due to irregular contact with quartz diorite in the vicinity

A strong type "B" response roughly correlates with the polarization high centered beneath stations 15 and 16. These spectra are probably generated by concentrations of pyrite. The type "b" responses that pervade the area are so flat that normal mineral discrimination procedures cannot be used. However, as mentioned in the discussion on line C, these spectra probably display the effects of sulfides, and most certainly include a response due to pyrite.

Line E

The apparent resistivity pseudosection shows the effects of near-surface low resistivity blocks centered beneath stations 11–12, 14–15, and 18 through 20. The blocks beneath 11–12 and 14–15 are also associated with low polarization values.

The andesite host to the east of station 12 provides relatively uniform type "B" responses. Spectra to the west of 12 are variable, reflecting complex geology in that area.

This line has provided stronger polarization and spectral responses than lines C and D, possibly showing a higher concentration of pyrite. The high frequency type "B" responses persist at depth beneath station 16, again indicating high concentrations of pyrite.
It is felt that differences in low frequency effects will help determine if mineral discrimination is possible.

As mentioned in the discussion on line C, it would be very helpful to obtain information on drillhole results and to be able to measure some selected core samples for correlation with field results in this area.

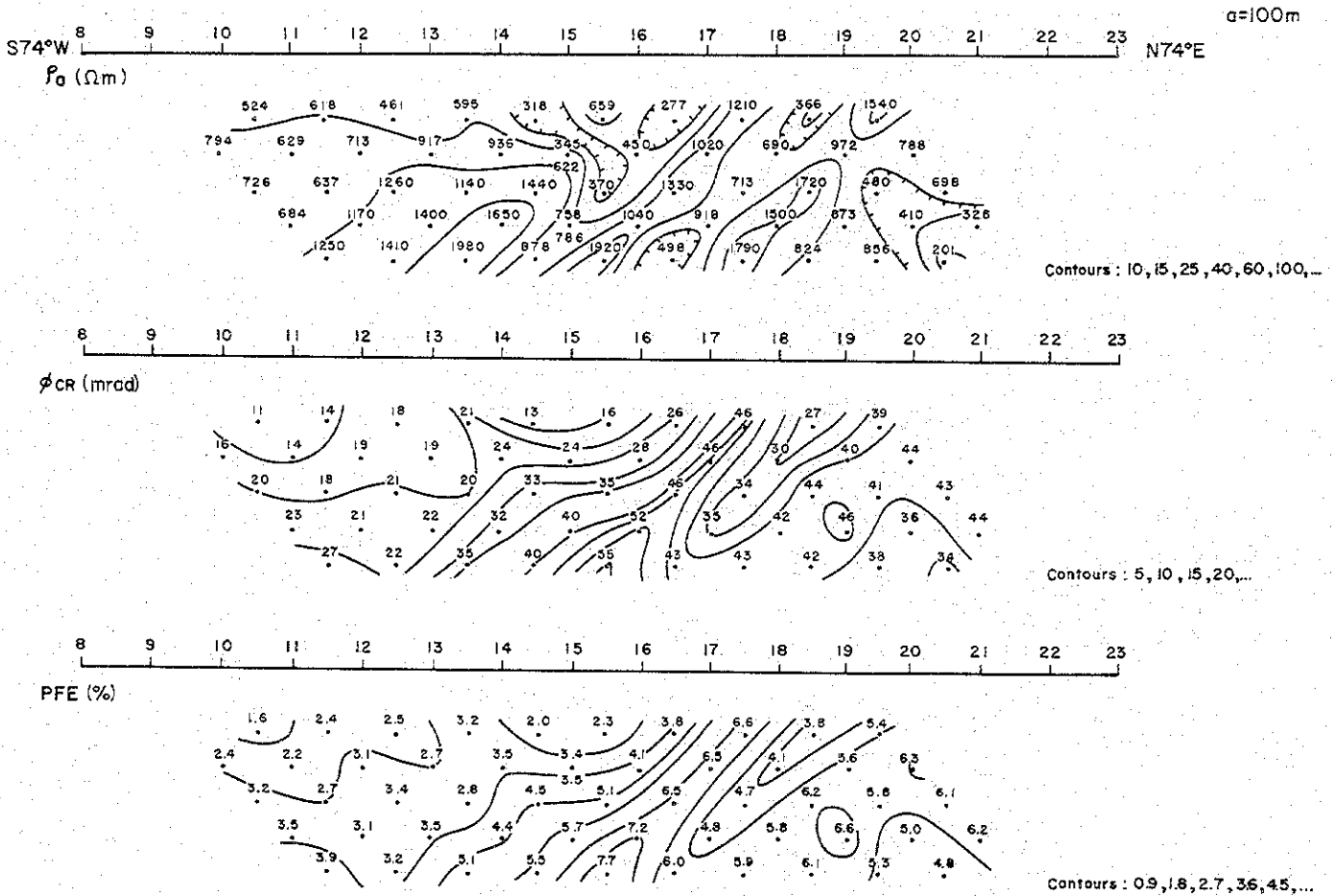

Fig. III–5–1 CR Profile (Line C)

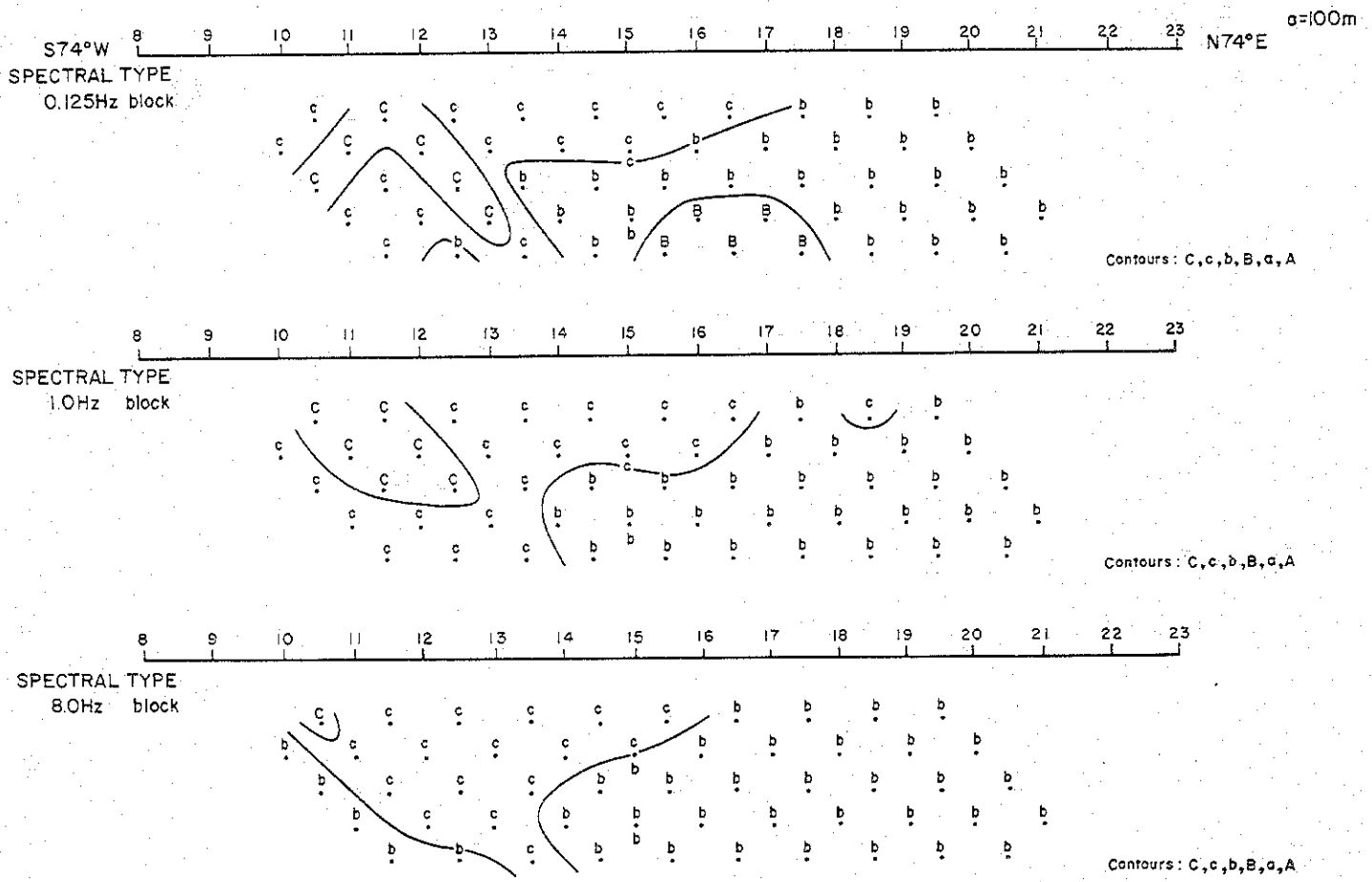

Fig. III–5–2 Spectral Profile (Line C)

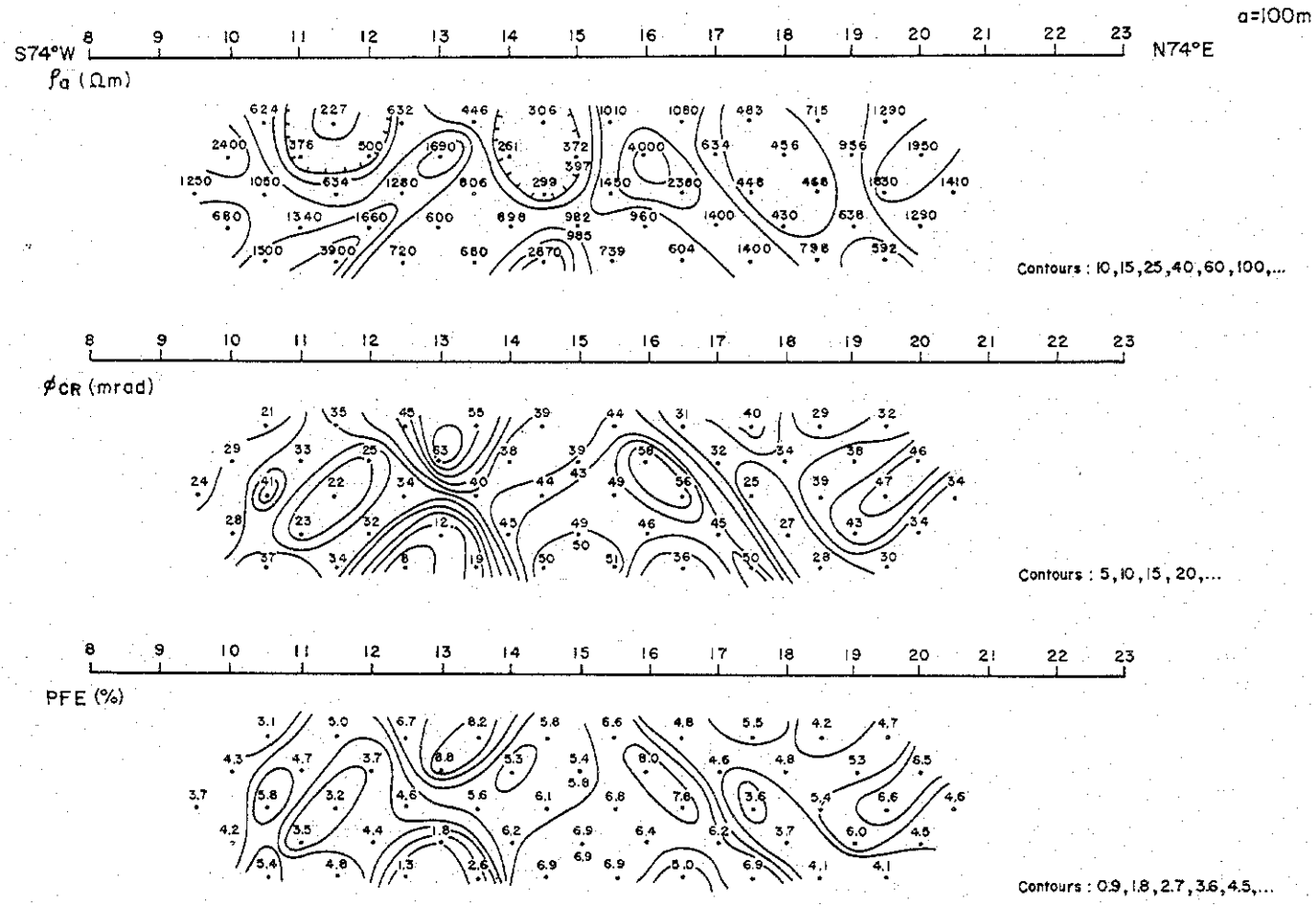

Fig. III–5–3 CR Profile (Line D)

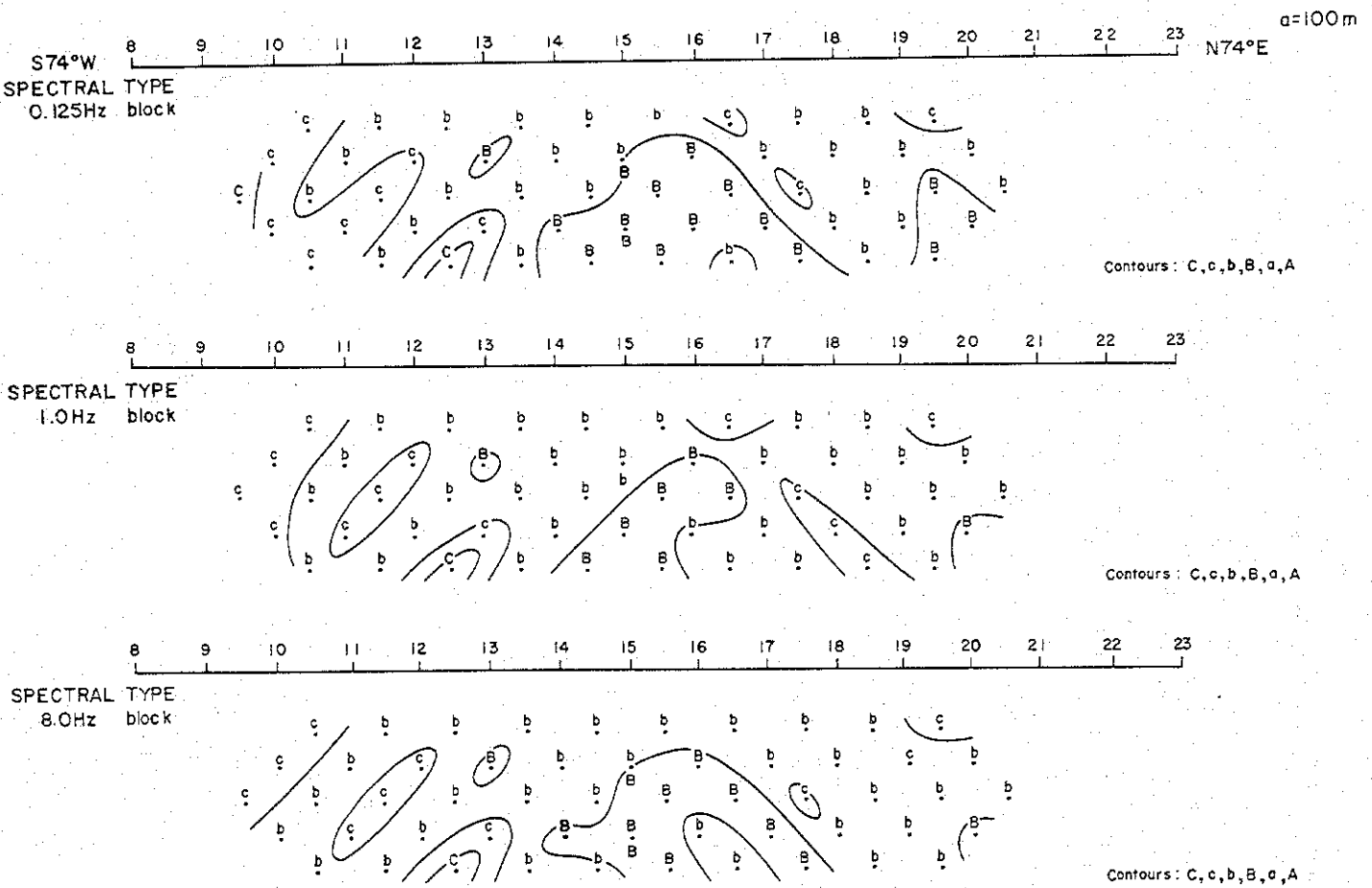

Fig. III–5–4 Spectral Profile (Line D)

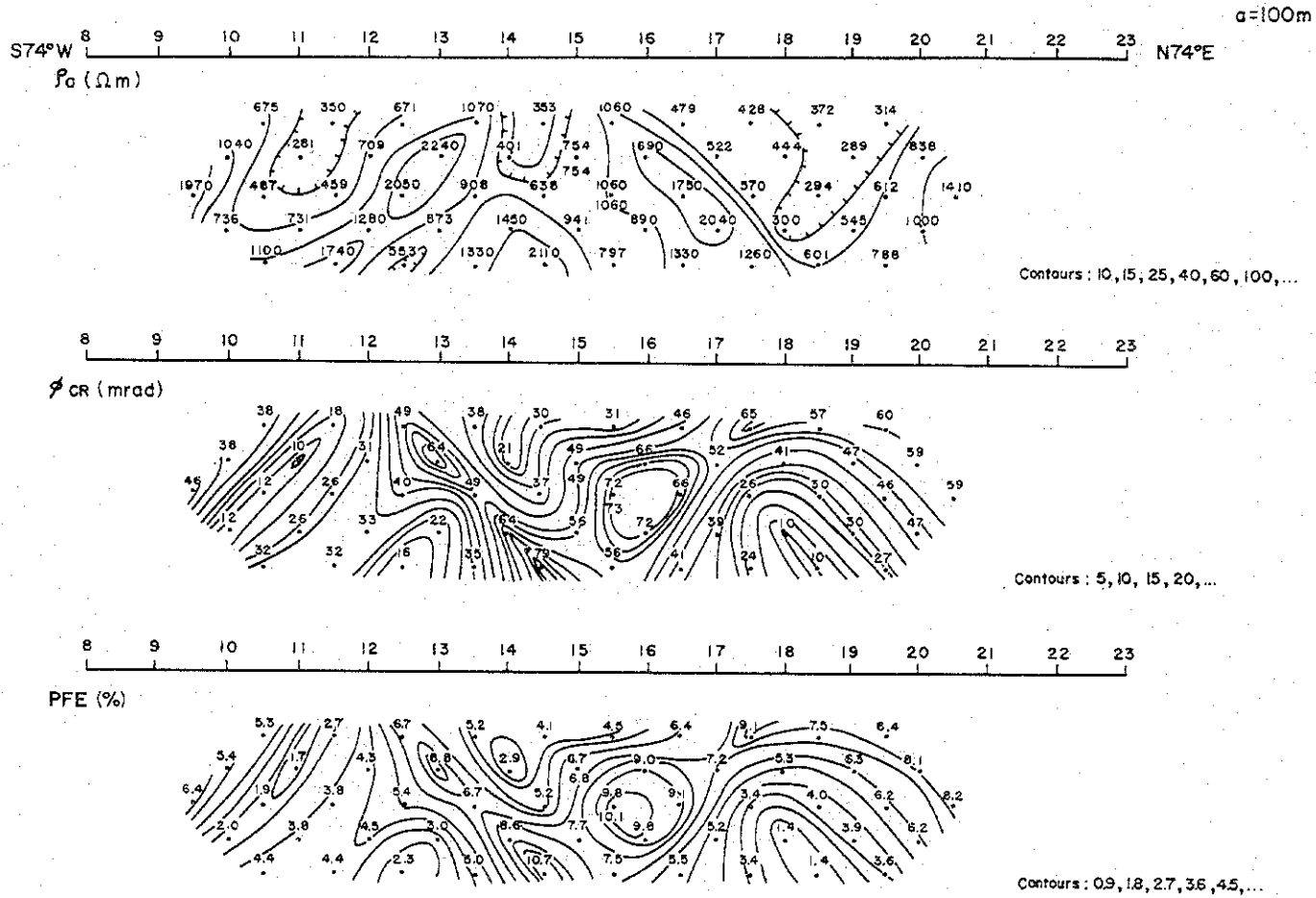

Fig. III–5–5 CR Profile (Line E)

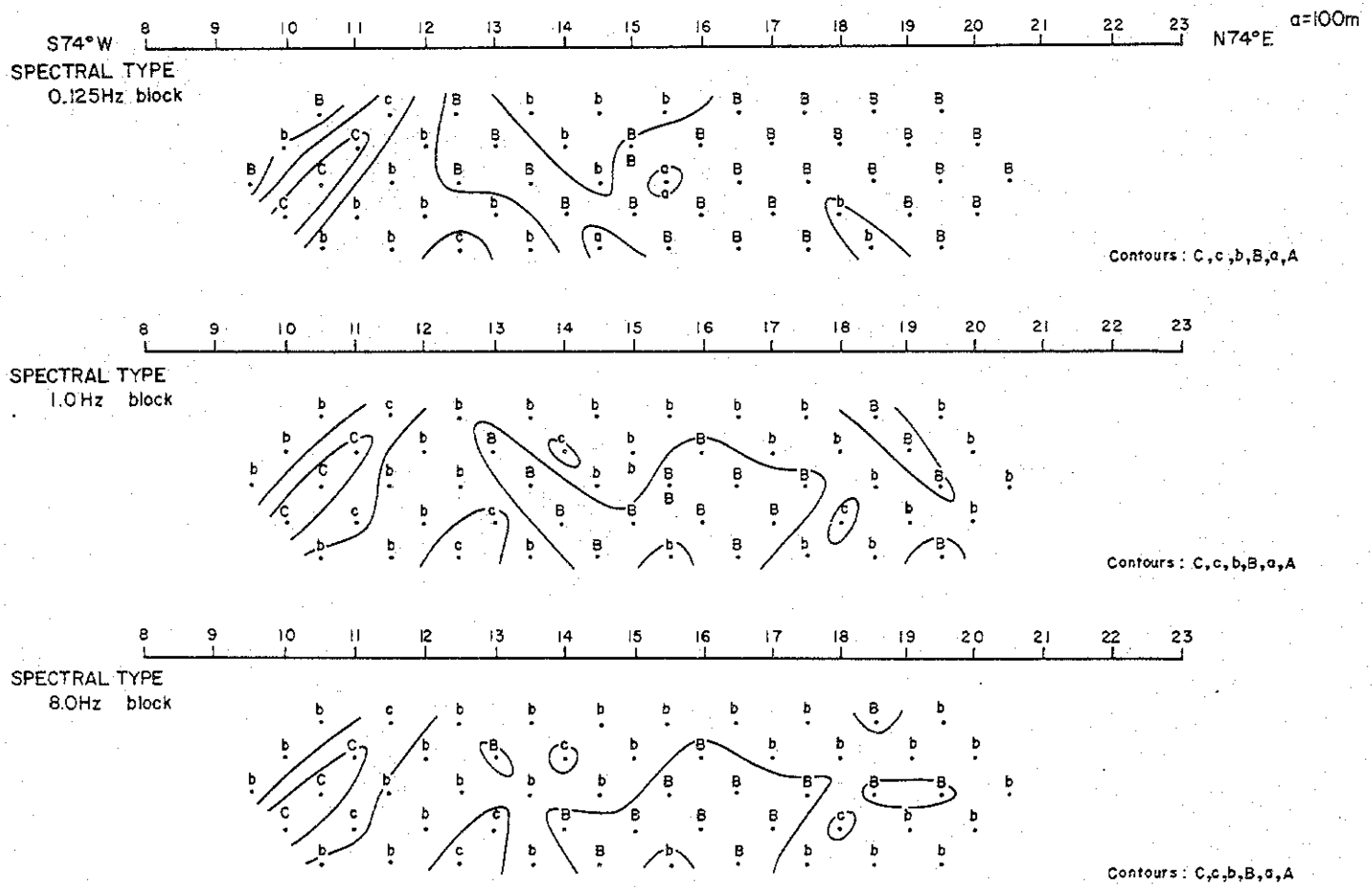

Fig. III–5–6 Spectral Profile (Line E)

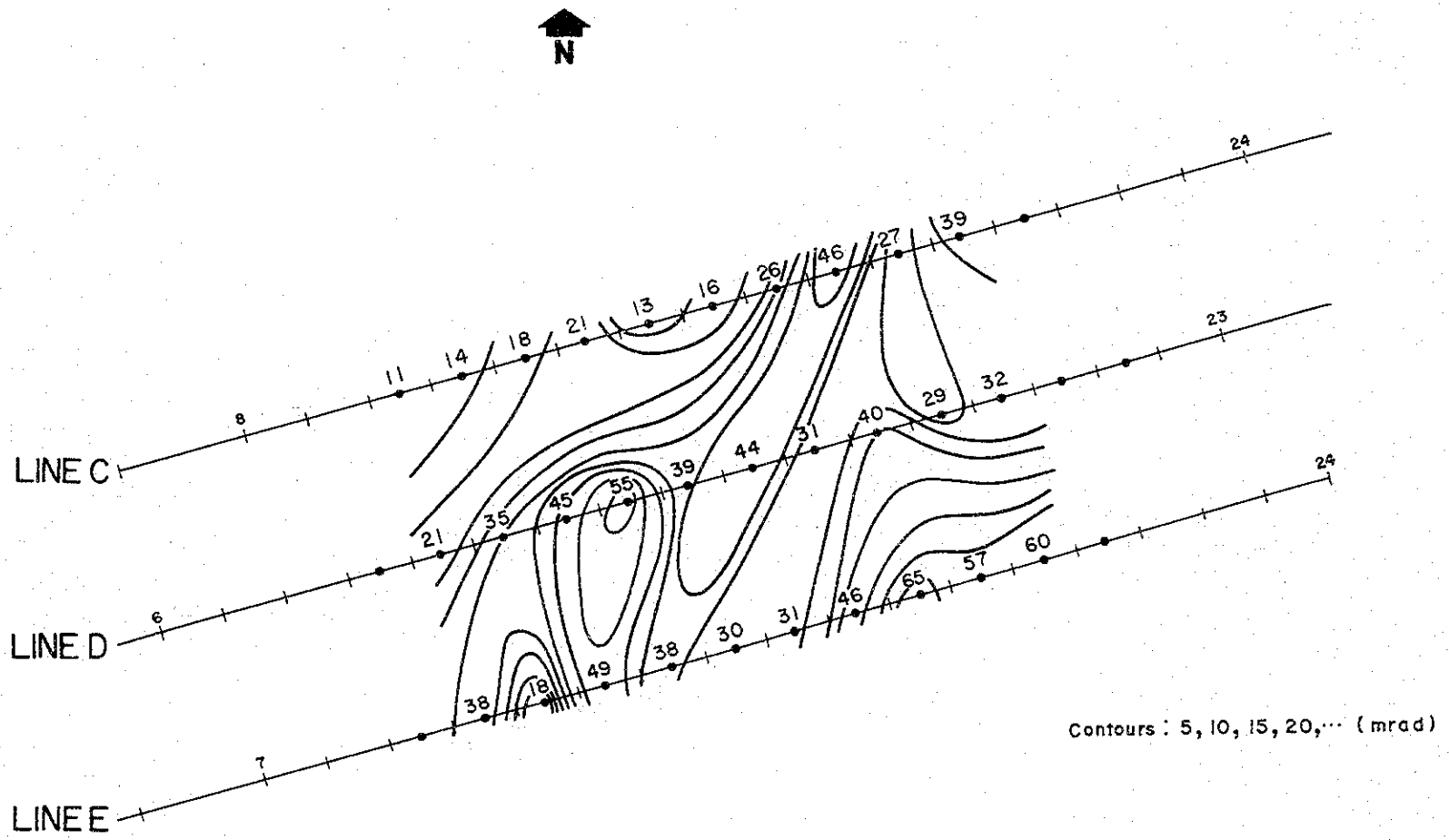

Fig. III–6–1 Apparent Polarization Map (n = 1)

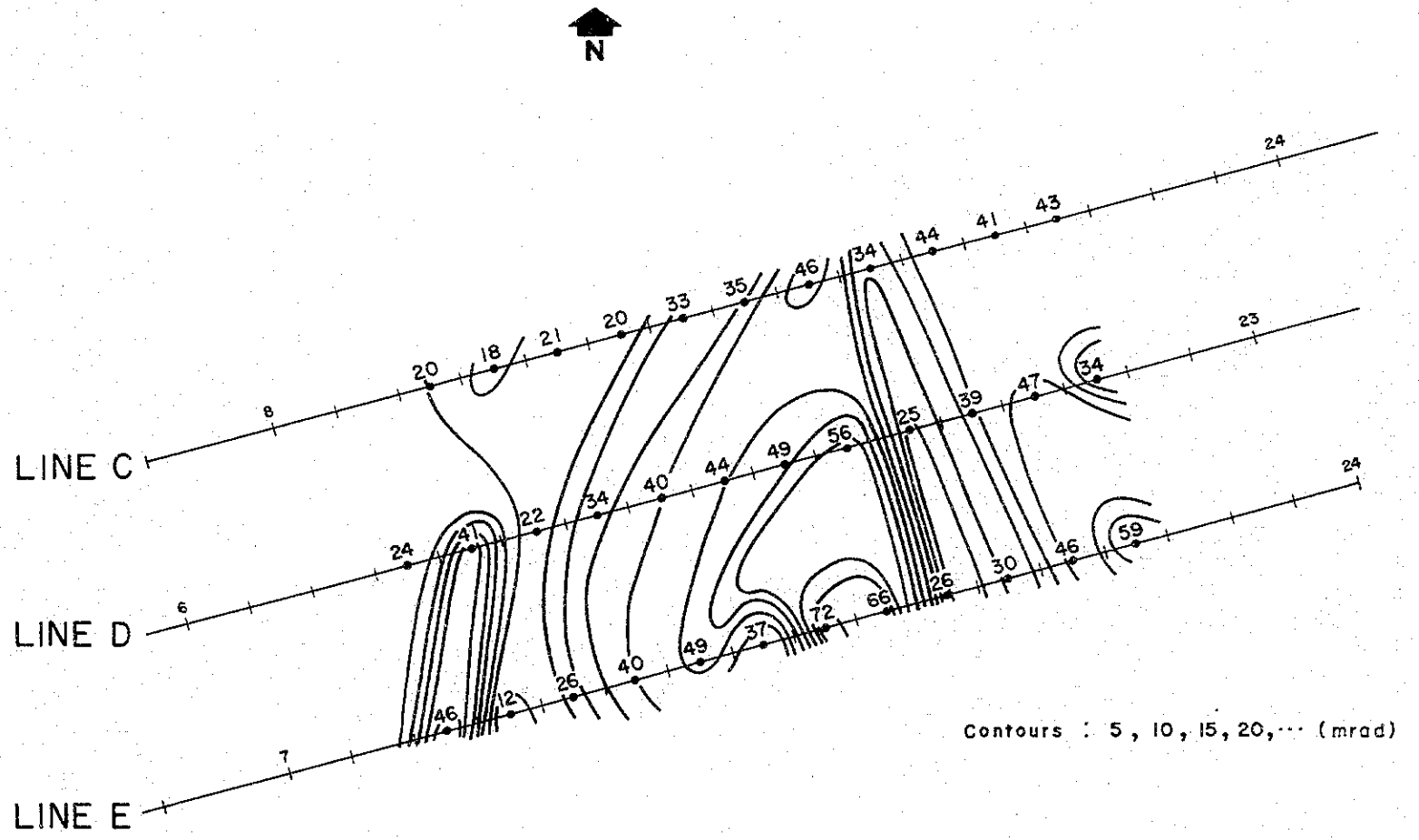

Fig. III–6–2 Apparent Polarization Map (n = 3)

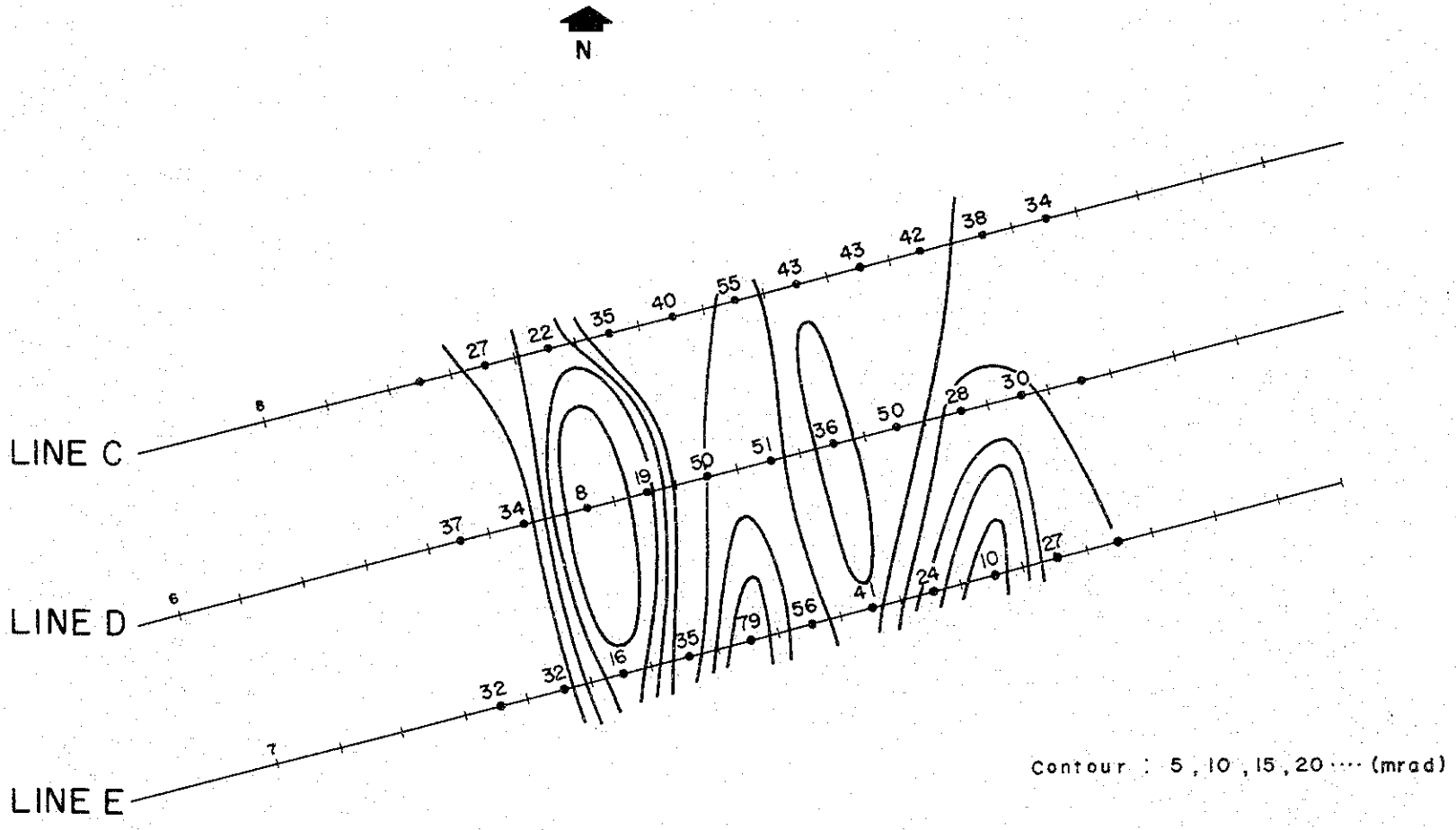

Fig. III–6–3 Apparent Polarization Map (n = 5)

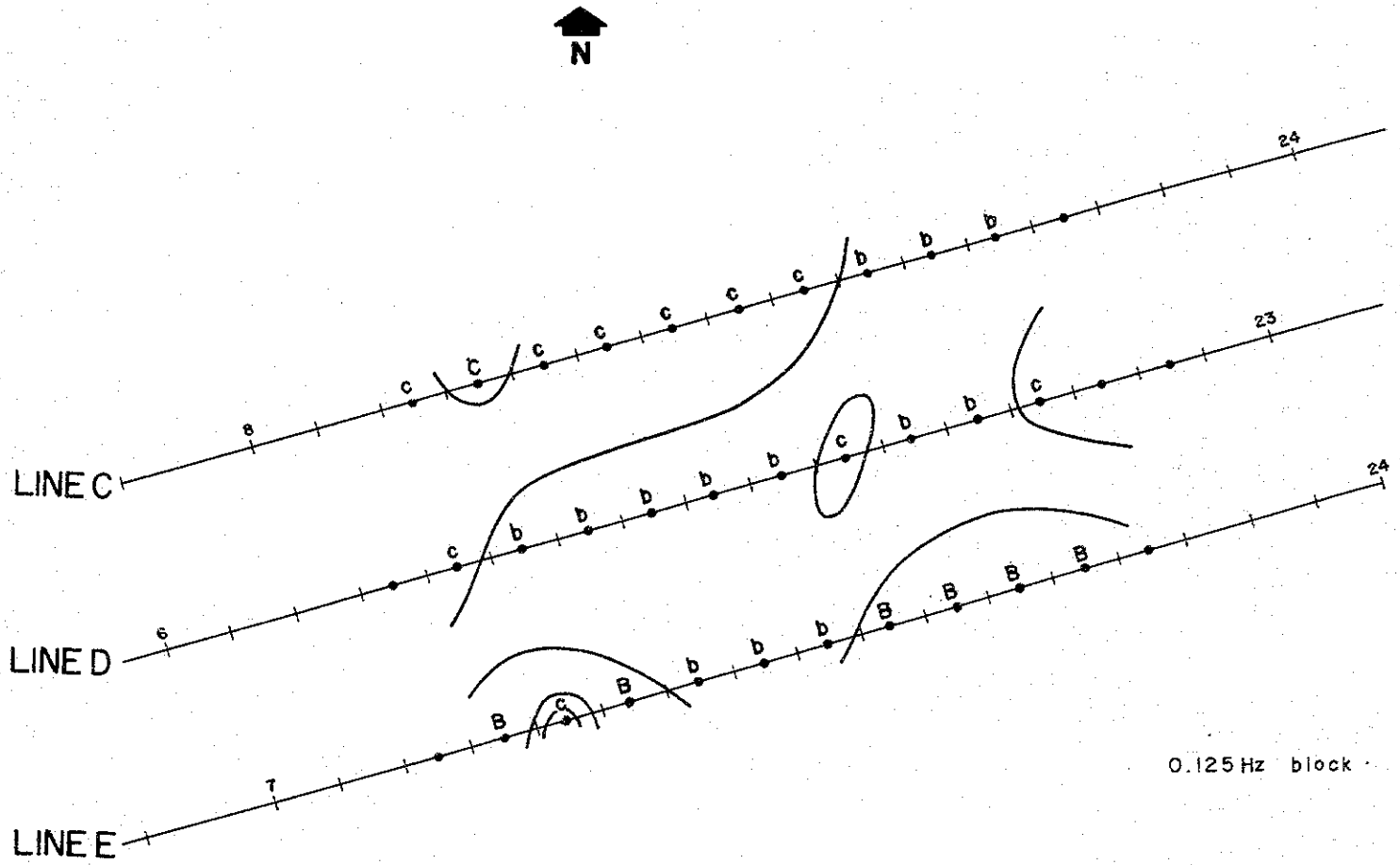

Fig. III–6–4 Spectral Type Map (n = 1)

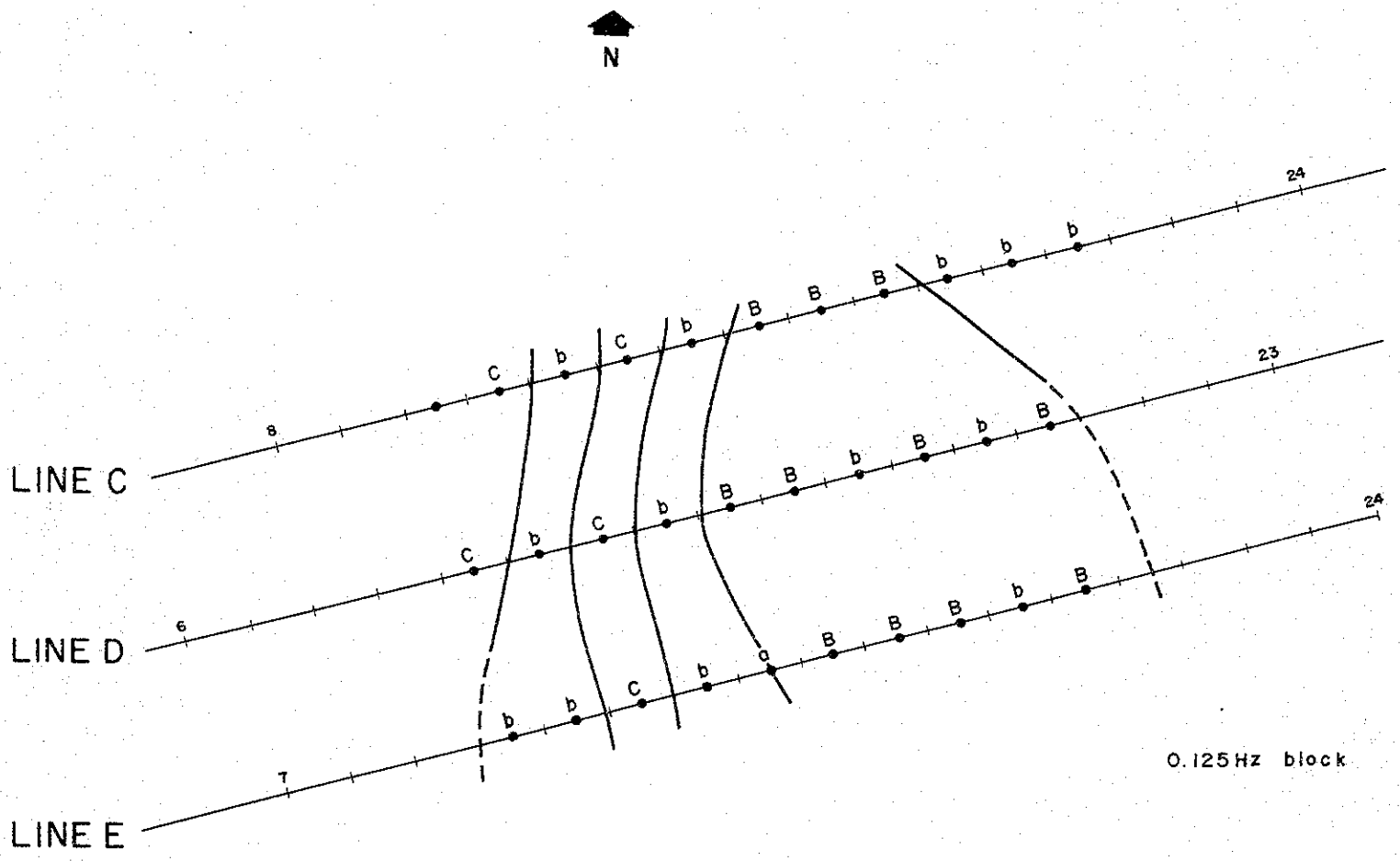

Fig. III–6–6 Spectral Type Map (n = 5)

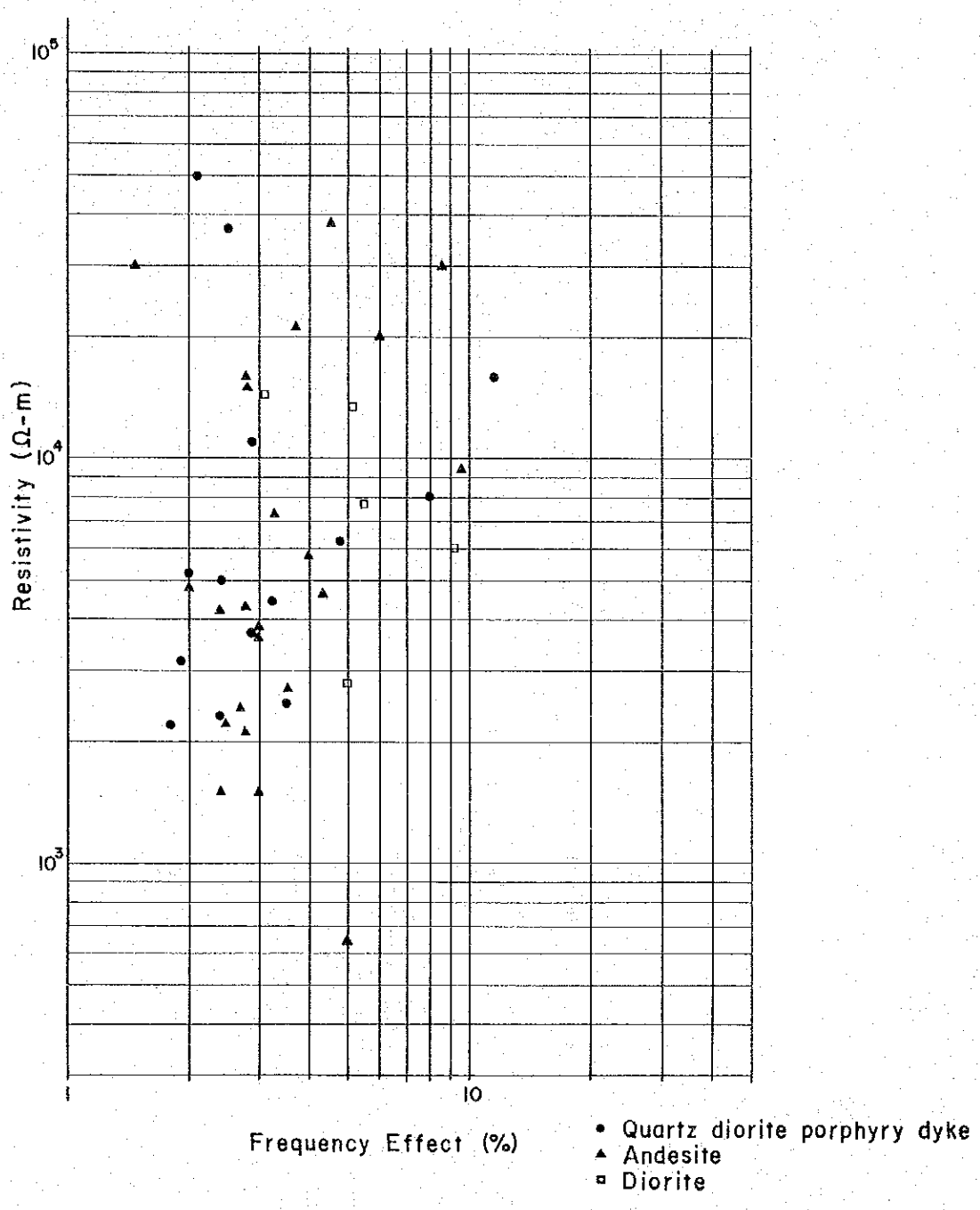

Fig. III–7 Correlation of Resistivity with FE

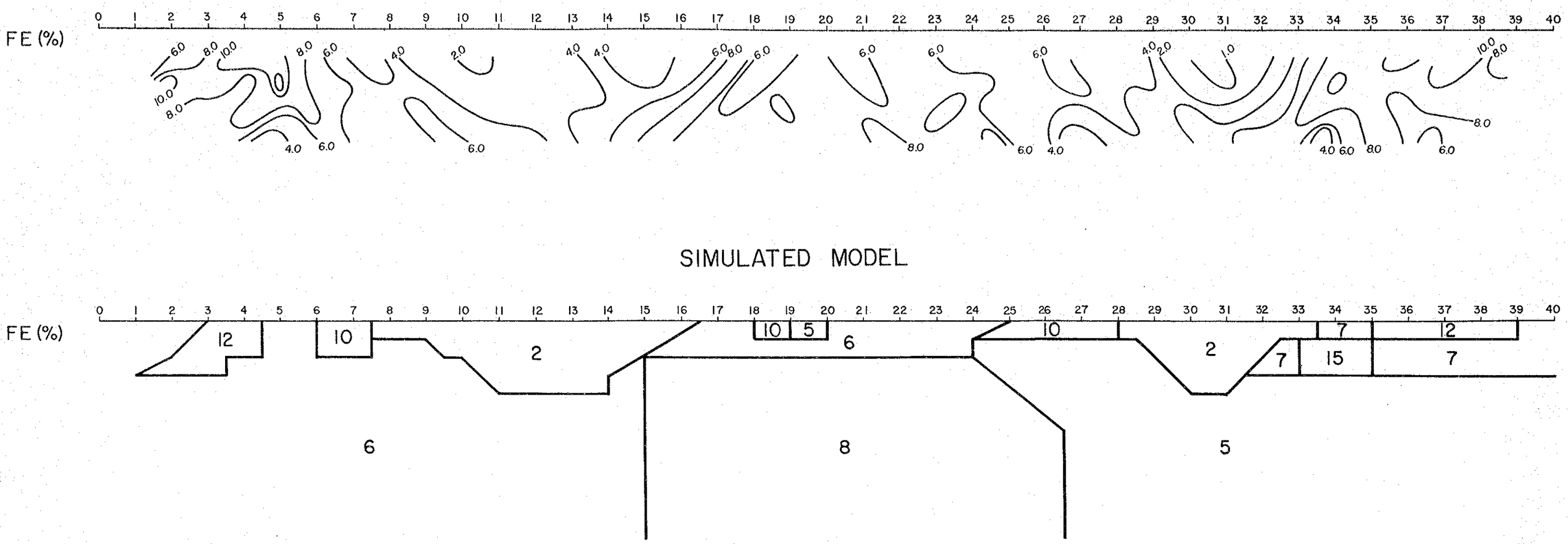

Fig. III–8–1 IP Model Calculation (Line C)

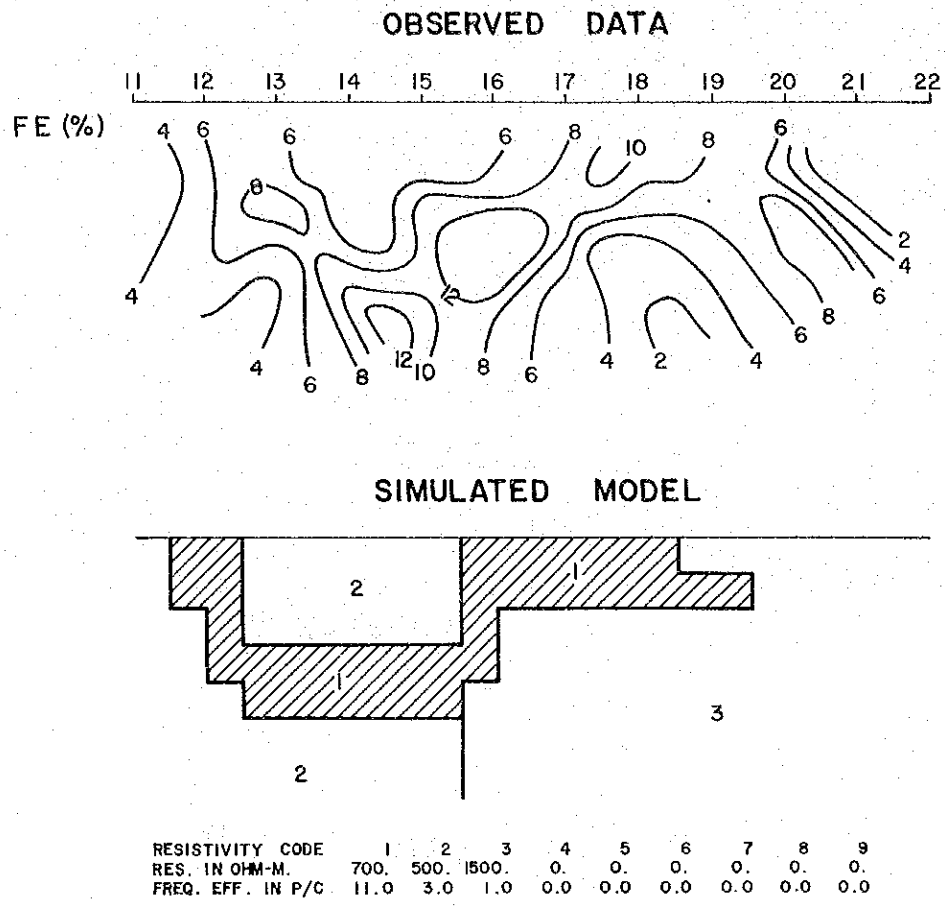

Fig. III–8–2 IP Model Calculation (Line D)

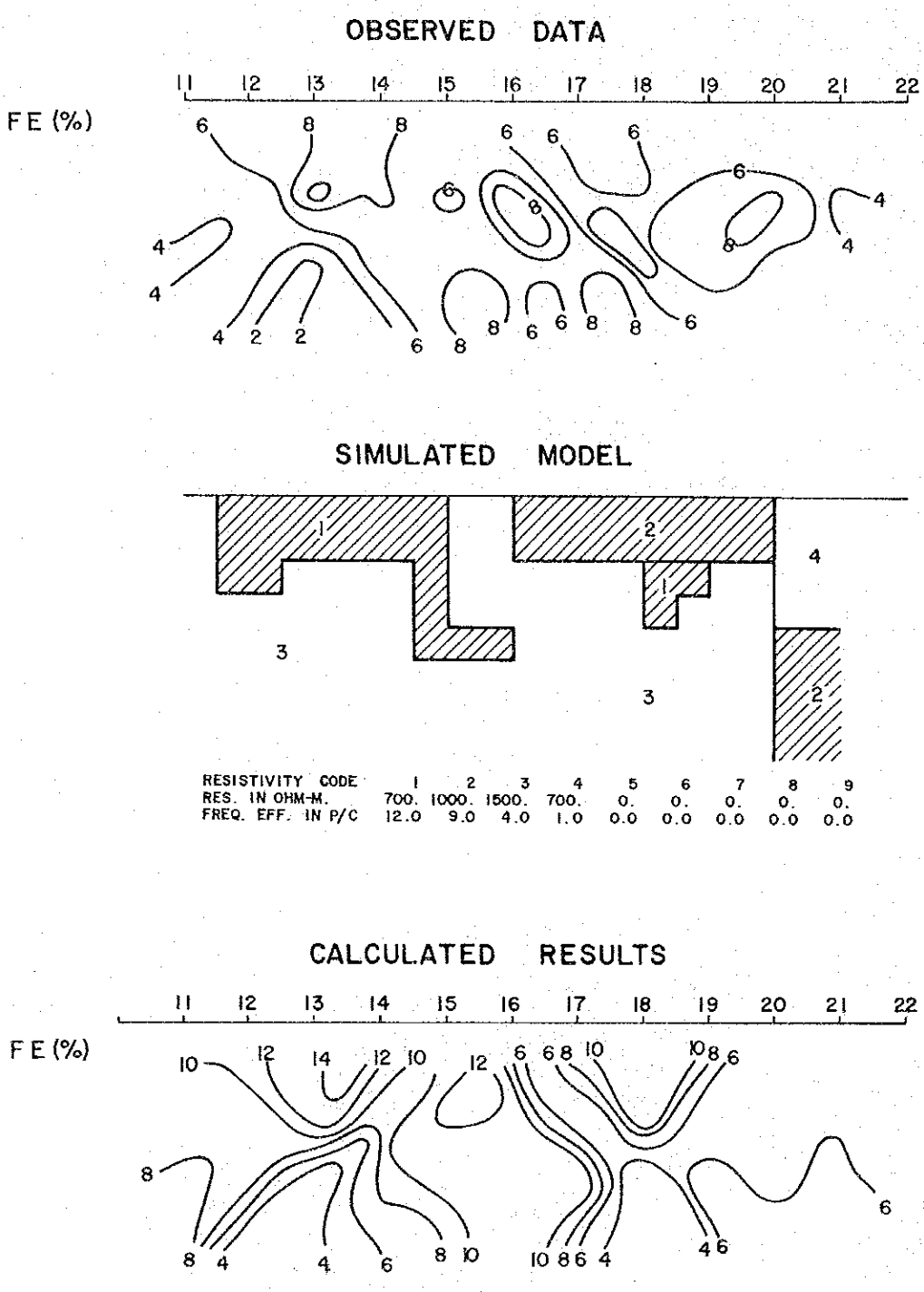

Fig. III–8–3 IP Model Calculation (Line E)

5. SUMMARY OF RESULTS

5–1 IP Method

The summary of results obtained from the IP method in the survey area is presented here.

The background FE in this area is about 3 percent, and above this value can be called an "Anomaly". Except the narrow area between the Western and Central anomaly zone mentioned earlier, and between the Central and Eastern anomaly zone, anomalies have been detected all over the area. It can be assumed from these results that the rocks in the survey area are undergoing some mineralization. Three anomalous zones of more than 5 percent FE have been observed in the area. They are referred to as the Western, Central and Eastern anomaly zones.

(A) The Western anomaly zone is distributed west of the Mamising River, with a N-S trend, it is centered at station 3 to 6 on Line C and D, and extends to the south and the north, and it also correlates with the low resistivity zone. However the intensity of FE anomaly decreases at increasing depth, in the N-S direction where the resistivity also becomes higher. The northern part of this anomaly zone is underlain by quartz diorite and granodiorite, while andesite lavas cover the southern part. The center of the anomaly zone coincides roughly with the contact between quartz diorite and andesite lavas. Where numerous small joints and fractures filled with pyrite and clay were observed. The copper mineralization was detected at the outer edge of this anomaly. From this it can be assumed that the network disseminated type mineralization of pyrite, concentrated near the surface is causing the anomaly. Mineralization diminishes at depths in the anomalous zone.

(B) The Central anomaly zone is widely distributed in a fan-shaped area extending north, starting from station 12 on Line G. This zone is the largest and from its pattern it tends to spread wider toward the north. The mineralization assumed from the magnitude of FE is weak in the south and locally on Line G, although a relatively large-scale mineralization is expected to extend from the surface to depth on Lines B, C, D and E. Drillholes RPJ-1, RPJ-2 and RPJ-3 which were performed at the central parts of the anomaly, indicate this anomaly to be due to network mineralization of pyrite occurring in andesite, correlating with the low resistivity zone which continues to greater depth. Andesite is widely distributed in this zone, and in its vicinity, quartz diorite and quartz diorite porphyry are recognized. This anomaly is located at the east margin and on the east side of the copper mineralization

along the Mamising River, and become strong in the region of the contact between andesite and quartz diorite. From the observation of the surface geology, most of the rocks in this vicinity undergo network mineralization, which is dominant in the contact between andesite and quartz diorite. Also, major joints and fractures filled with quartz, pyrite and occasionally clay are observed in the andesite. The strong FE anomaly is assumed to be induced by the above mentioned pyrite mineralization concentrated along the boundary between the andesite.

(C) The Eastern anomaly zone is distributed east of station 32 of each Line, except Lines A and G. The scale of the anomaly zone is small compared with the Central anomaly zone, but the highest FE value was observed here. The distribution of the anomaly, possibly coincides with the disseminated and vein type mineralization of quartz diorite which crops out east of Nagasasan. It is the strongest on Line B and becomes weaker and smaller towards the south. The strongest area fits very closely to the low resistivity zone. As copper minerals are not found in quartz diorite from the surface geology, it is assumed that this anomaly may be due to the pyrite concentration along the fissures of the quartz diorite, extending to depth of Lines B, C and D.

5–2 Complex Resistivity Method

All three lines on this survey provide high polarization values and relatively uniform, flat spectral responses "c" and "B".

The overall intensity of polarization and spectral response increases toward the south, with Line E being the most responsive. Complex resistivity measurements on rock samples show the type "A" and "a" response, and 25 percent FE in the sample with abundant pyrite/chalcopyrite, while the type "C" and "b" and FE less than 3 percent, are present in host rock such as andesite and quartz diorite.

Compared with the results of IP survey, type "B" and "b" response roughly coincide with the Central anomaly zone. It is relatively certain that the type "B" and "b" responses are probably due to large concentrations of pyrite in andesite and quartz diorite.

The type "C" and "c" response on the west end of each line correlates with the geochemical Cu – anomaly distribution, but measurements on rock samples show type "C" and "c" to be due to the non-mineralized host rock. The reason for this contradiction of geochemical anomaly with spectral response is probably due to the secondary oxidation of copper sulfides.

However, as drillholes RPJ-1 (station 15 on Line C) and BM.3 (station 10 on Line C) detect the mineralization of copper in the order of 0.2 to 0.4 percent by weight, copper sulfides (Chalcopyrite) are expected to be present underground.

With a new analysis method utilizing correlation of phase difference with frequency by M.M.A.J., a different type of response has been detected in the area of type "C" response.

It is necessary to investigate further whether this detection suggests the existence of disseminated mineralization of copper, and only a classification of "A", "a", "B", "b", "C" and "c" as determined by ZERO is not enough in the search for the sulfide deposits of economical interest. It is desirable to establish a new basis for evaluating the significance of CR results.

PART Ⅳ DRILLING EXPLORATION

1. GENERAL REMARKS

The drilling exploration being a part of the phase III survey of this project was conducted in the Manikbel area where was delineated as the most promising area for ore deposits from the phase I and II surveys. The purpose of this exploration is to confirm the extent of the mineralized zone consisting of disseminated pyrite and secondary copper minerals and to test the IP anomalous zone detected along the eastern margin of the mineralized zone. For these purposes, three holes, 932.20 m in total length, were drilled in the eastern portion of the Mamising Creek as shown in Fig. IV–1.

The drilling operations were carried out in three shifts with wireline method using only one set of drilling machine from the begining of January to the end of March, 1981. The operations went on smoothly, and average drilling length per shift is 9.32 m with 98.3 % core recovery.

The details of the drilling operation and its results are described hereafter.

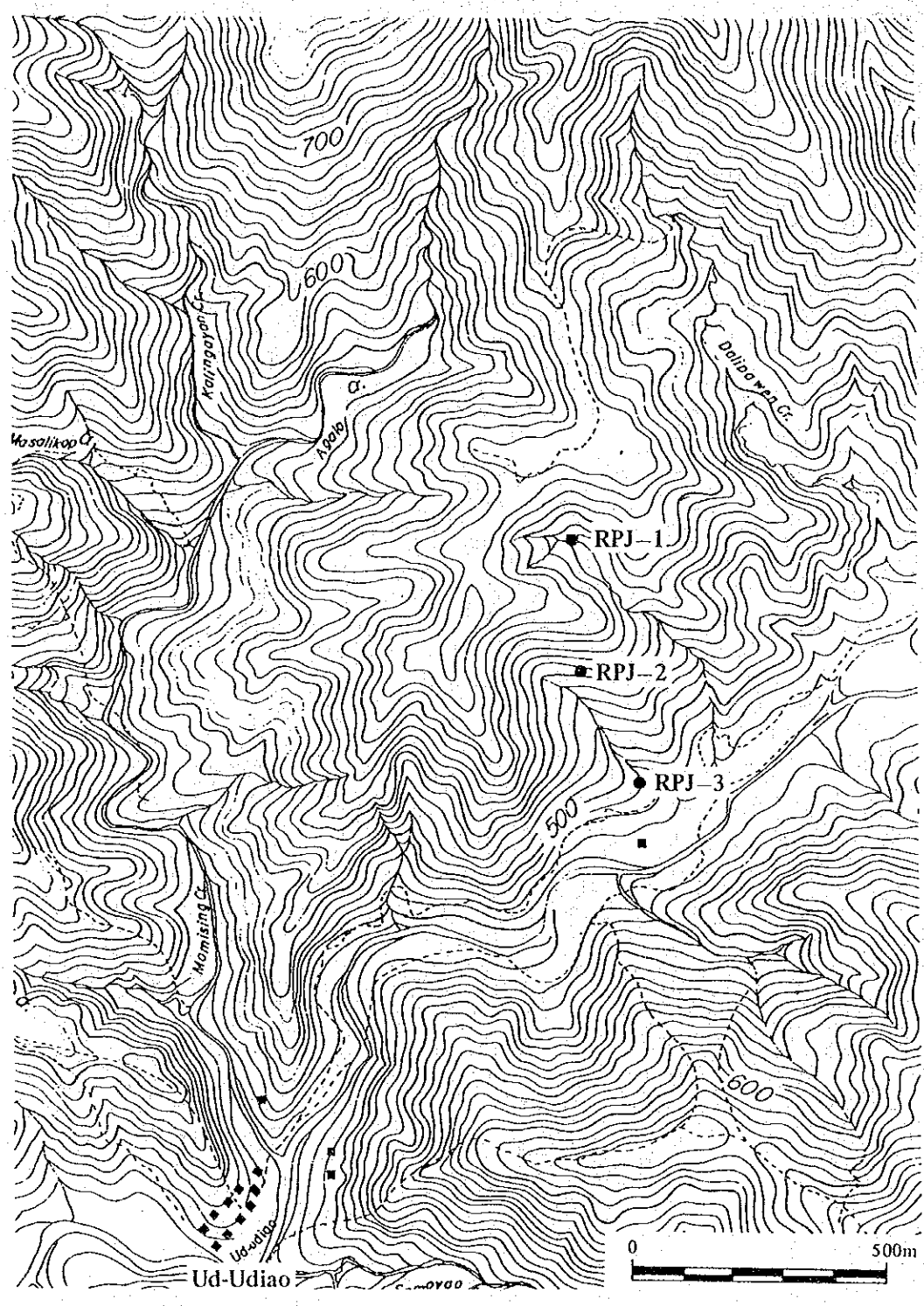

Fig. IV-1 Location Map of Drilling Sites

2. DRILLING METHOD AND DRILLING MACHINE

From the information and data on the drilling exploration in the area, it was expected that drill holes will encounter several sheared and/or fractured zones. The drilling method, therefore, was designed for the improvement of core recovery, prevention of water circulation loss and reduction of drilling friction.

Three size tools of HQ, NQ and BQ were prepared, but drilling of each hole was commenced and ended by HQ and NQ because of stable condition of hole-wall.

The types and specifications of the machine used are shown in Table IV–1.

Table IV–1 Drilling Equipment and Consumed Materials

A. Model "TGM-2C"

Article	Model	Specifications	Quantity
Drilling Machine	Model "TGM-2C" (Tone Boring, Co.)	Capacity: BQ-WL 550 m Dimensions: Height 1,520 mm Length 2,430 mm Width 0.990 mm Weight (without Power Unit): 1,200 kg	1 set
	Swivel Head	Spindle Speed: 140 340 530 700 r.p.m.	
	Hoist	Type: Planetary Gear Type (Power Up) Capacity: 4,500 kg	
	Oil Pump	Type: Gear Type, Two-steps Variable Delivery Vane Type capacity: 60 /min Pressure: Max. 30 kg/cm^2 Ord. 20 kg/cm^2	
Motor	Model "F4L-912" (Mitsui Deuts, Co.)	Diesel Engine: 4 Cycle Air-cool Type Revolution: 1,500 ~ 2,000 r.p.m. Related Power: 31.5 ~ 41 P.S.	1 set
Drilling Pump	Model "NES-4" (Tone Boring, Co.)	Duplex Cylinder Double Action Weight (without Power Unit): 325 kg Piston Diameter: 60, 70 mm Stroke: 50 mm Max. Capacity: 71, 100 /min Max. Pressure: 50, 35.5 kg/cm^2	1 set
Water Supply Pump	Model "NS-110"	Diesel Engine (Yanmer Diesel Co.) Revolution: 2,200 r.p.m. Related Power: 11 P.S.	1 set
Derrick	Iron Square Pot Type	DRP-9-5	1 set
Drill Rod		HQ – 3 m HQ – 1.5 m NQ – 3 m NQ – 1.5 m	45 pcs 1 pc 110 pcs 1 pc
Casing Pipe		HW – 3 m HW – 1 m NX – 3 m NX – 1 m NX – 0.5 m	10 pcs 1 pc 50 pcs 10 pcs 5 pcs
Wireline Hoist		Attached to Drilling Machine	1 set
Rod Safety Clamps		RH-85 Type	1 set
Water Swievel		DH Type	1 set
Travelling Block			15 pcs
Hoisting Swivel		B Type	1 set

B. Consumed Materials

Article	Specification	Unit	Quantity			
			RPJ–1	RPJ–2	RPJ–3	Total
Gasoline	Jeep	L	700	440	390	1,530
Light Oil	Engine	L	1,400	880	1,400	3,680
Mobil Oil	Engine	L				200
Mission Oil	Gear	L				60
Turbine Oil	Oil Pressure	L	80	50	80	210
Grease		kg				60
Cutting Oil			400	300	300	1,000
Metal Crown	HX	pcs				5
Single Core Tube	116 m/m x 0.5 m	set				1
Double Core Tube	HQ-WL	set				2
do	HQ-WL	set				3
Wire Cutter	12 m/m	pg				1
Core Tube Head	HX	pcs				1
Casing Head	HX	pcs				1
do	NX	pcs				1
Casing Metal Shoe	112 m/m	pcs				1
do	HX	pcs				3
do	NX	pcs				3
Cement		pack	5	4	4	13
Rag		kg				60
Core Box		pcs	50	52	53	155
Board	20 m/m	m^3				3
Wire	#10	kg				100
do	#12	kg				100
Nail	75 m/m	kg				30
do	38 m/m	kg				30
Wire Rope	19 m/m x 1000 m	vol				1
do	10 m/m x 1000 m	vol				1
Manila Rope	19 m/m x 100 m	vol				2
do	19 m/m x 50 m	vol				2
Binyl Rope	8 m/m x 250 m	vol				2
V-Belt	Engine	set	2	2	2	6
do	Pump	set	2	2	2	6
Wire Rope	5 m/m x 350 m	vol				2
Core-Lifter	HQ-WL	pcs				10
do	HQ-WL	pcs				15
Core-Lifter Case	HQ-WL	pcs				5
do	NQ-WL	pcs				8
WL-Accessary	HQ-WL	set				1
	NQ-WL	set				1
Working Dress	M, L	set				18
Working Gloves		pair				84
Lighting Fixture	12 V – 60 W	set				20
Working Shoes	25 ~ 27 cm	pair				10
Pressure Gauge	100 kg/cm^2	pcs				3
Bentnite		tt	0.4	0.3	0.3	1.0

C. Consumed Bits

Bit Type		RPJ–1		RPJ–2		RPJ–3		Total	
		Drilled Length	Quantity	Drilled Length	Quantity	Drilled Length	Quantity	Drilled Length	Quantity
HX Single	Bit	18.00 m	1.0 pcs	15.00 m	1.0 pcs	17.00 m	1.0 pcs	47.00 m	3.0 pcs
	Reamer	18.00	0.4	15.00	0.3	17.00	0.3	47.00	1.0
HQ–WL	Bit	56.95	2.0	78.00	3.0	94.40	4.0	228.95	9.0
	Reamer	56.95	0.5	78.00	0.5	94.40	1.0	228.95	2.0
NQ–WL	Bit	235.05	9.0	217.90	8.0	199.90	8.0	652.85	25.0
	Reamer	235.05	2.0	217.90	2.0	199.90	2.0	652.85	6.0